STUDY OF ISOTHERMAL PRESSURE DROP AND NON-BOILING HEAT TRANSFER IN VERTICAL DOWNWARD TWO PHASE FLOW

By

MEHMET MOLLAMAHMUTOGLU

Bachelor of Science in Mechanical Engineering

Gazi University

Ankara, Turkey

2009

Submitted to the Faculty of the
Graduate College of the
Oklahoma State University
in partial fulfillment of
the requirements for
the Degree of
MASTER OF SCIENCE
December, 2012

STUDY OF ISOTHERMAL PRESSURE DROP AND NON-BOILING HEAT TRANSFER IN VERTICAL DOWNWARD TWO PHASE FLOW

Thesis Approved:

Dr. Afshin Ghajar
Thesis Adviser

Dr. Khaled Sallam

Dr. Frank Chambers

Dr. Sheryl Tucker
Dean of Graduate College

Name: MEHMET MOLLAMAHMUTOGLU Date of Degree: Dec, 2012

Institution: Oklahoma State University Location: Stillwater, Oklahoma

Title of Study: STUDY OF ISOTHERMAL PRESSURE DROP AND NON-BOILING HEAT TRANSFER IN VERTICAL DOWNWARD TWO-PHASE FLOW

Pages in Study: 97 Candidate for the Degree of Master of Science

Major Field: Mechanical Engineering

Scope and Method of Study: In the present study, two phase flow pressure drop and non-boiling heat transfer in downward orientation was investigated experimentally. Air-water mixture was used as working fluids and the inner diameter of the pipe was 0.01252 m. As a result of experimental work, a detailed analysis based on flow patterns was made to enlighten hydrostatic and heat transfer characteristics of two phase flow in downward orientation, and also possible effects of buoyancy on the flow. In addition, the data was tested against some of the best known correlations in the literature and the performance analysis of the correlations was also given. Based on the efficiency of the correlations, possible reasons were discussed and some recommendations were made for further works.

Findings and Conclusions: The experimental results verified other researchers' findings that inclination had a major influence on two-phase flow. Both pressure drop and heat transfer data showed that the pressure drop and heat transfer characteristics of downward flow were greatly dependent on flow patterns. The slug and the falling film regimes were the most distinctive ones due to their unpredictable behaviors. Briefly, very non linear trends and generally high frictional pressure drop and heat transfer values were observed. Therefore, the efficiency of available two phase correlations was limited to the flow patterns. The heat transfer correlations were able to produce more reasonable results for the entire experimental data. On the other hand, the pressure drop correlations failed for the entire range except the bubbly and annular flow regimes. As a result, it was seen that different approaches were needed to develop robust correlations in order to find a general solution for both pressure drop and heat transfer phenomena. Fortunately, a consistent relation between heat transfer and pressure drop data was seen. Thus, a good pressure drop model would also provide a solution for the heat transfer case due to the Reynolds analogy.

ADVISER'S APPROVAL: Dr. Afshin J. Ghajar

ACKNOWLEDGMENTS

I would like to thank to my advisor Dr. Afshin Ghajar for his support, motivation and patience during this study. I also would like to thank my thesis committee, Dr. Frank Chambers and Dr. Khaled Sallam for their valuable recommendations.

I would like to give special thanks to our former research group member Dr. Clement Tang for his help and other members of our research group for their friendship during the study.

I am also grateful to my father, my mother and my brother for their support during my education in USA.

TABLE OF CONTENTS

Chapter Page

I. INTRODUCTION 1

II. REVIEW OF LITERATURE 4

2.1 Pressure Drop 4
2.2 Heat Transfer 11

III. EXPERIMENTAL SETUP 14

3.1 Details of Experimental Setup 16
3.2 Data Acquisition System 21
3.3 Experimental Procedure 21
3.3.1 Pressure Drop Measurements 21
3.3.2 Heat Transfer Measurements 25
3.4 Data Acquisition 26
3.5 Validation of Experimental Setup 27
3.5.1 Single Phase Pressure Drop Measurements 27
3.5.2 Single Phase Heat Transfer Measurements 28

IV. RESULTS AND DISCUSSION 31

4.1 Pressure Drop 31
4.1.1 Analysis Based on Flow Patterns 33
4.1.2 Performance of Correlations for Pressure Drop Results 45
4.2 Heat Transfer 51
4.2.1 Analysis Based on Flow Patterns 52
4.2.2 Performance of Correlations for Heat Transfer Results 59
4.2.3 Comparison of Heat Transfer Characteristics of Downward and Upward Orientations 65
4.3 Recommendations for Modeling 66

V. CONCLUSIONS AND RECOMMENDATIONS 75

5.1 Conclusions of Pressure Drop Measurement and Analysis 76
5.2 Conclusions of Heat Transfer Measurement and Analysis 77
5.3 Recommendations for Future Experimental Pressure Drop Studies.....79
5.4 Recommendations for Future Experimental Heat Transfer Studies 81

REFERENCES 83

APPENDIX A UNCERTAINTY ANALYSIS.....88

A.1 Pressure Drop.....88
A.1.1 Single Phase Flow.....88
A.1.2 Two-Phase Flow 89
A.2 Heat Transfer.....94

LIST OF TABLES

Table Page

Table 2.1 Homogeneous Pressure Drop Correlations 7
Table 2.2 Separated Flow Pressure Drop Correlations 9
Table 2.3 Two-Phase Flow Heat Transfer Correlations 12
Table 3.1 Recommendations for Two-phase Heat Transfer Measurements 26
Table 3.2 Single Phase Heat Transfer Correlations 29
Table 4.1 Performance Analysis of Various Heat Transfer Correlations against Data from Various Flow Patterns 60
Table A.1 Uncertainty Values Related to the Parameters 89
Table A.2 Single Phase Pressure Drop Sample Calculation (Run 0001, Re_{SL} = 34238) 89
Table A.3 Frictional Pressure Drop Uncertainties Based on Different Flow Patterns 92
Table A.4 Two Phase Pressure Drop Sample Calculations (Run 0004, Bubbly Flow) 93
Table A.5 Single Phase Heat Transfer Sample Calculations (Run=0001) 96
Table A.6 Two Phase Heat Transfer Sample Calculations (Run=0048, Slug Flow) 96
Table A.7 Two Phase Heat Transfer Uncertainties Based on Flow Pattern 97

LIST OF FIGURES

Figure Page

Figure 3.1 Schematic of Experimental Setup 15
Figure 3.2 Photograph of Experimental Setup and Schematic of Flow Visualization and Void Fraction Sections.....17
Figure 3.3 Schematic of Heated Section.....18
Figure 3.4 Water Mass Flow Meters.....19
Figure 3.5 Air Mass Flow Meters.....20
Figure 3.6 Schematic of Two Manometers System.....23
Figure 3.7 Schematic of Differential Pressure Transducer System.....24
Figure 3.8 Single Phase Pressure Drop Measurements against Colebrook-White Equation.....28
Figure 3.9 Single Phase Heat Transfer Measurements against the Correlations.....30
Figure 4.1 Variation of Frictional Pressure Drop against Re_{SG} in Bubbly Flow Regime.....34
Figure 4.2 Variation of Frictional Pressure Drop against Liquid Hold-up in Bubbly Flow Regime.....35
Figure 4.3 Variation of Frictional Pressure Drop Multiplier against Liquid Hold-up in Bubbly Flow Regime.....36
Figure 4.4 Variation of Frictional Pressure Drop against Re_{SG} in Slug Flow Regime.....37
Figure 4.5 Variation of Two-Phase Friction Factor against Liquid Hold-up in Slug Flow Regime.....37
Figure 4.6 Variation of Liquid Pressure Drop Multiplier against Liquid Hold-up in Slug Flow Regime.....38
Figure 4.7 Variation of Frictional Pressure Drop against Re_{SG} in Froth Flow Regime.....39
Figure 4.8 Variation of Frictional Pressure Drop against Liquid Hold-up in Froth Flow Regime.....39
Figure 4.9 Variation of Liquid Pressure Drop Multiplier against Liquid Hold-up in Froth Flow Regime.....40
Figure 4.10 Variation of Two-Phase Friction Factor against Liquid Hold-up in Froth Flow Regime.....41
Figure 4.11 Variation of Frictional Pressure Drop against Re_{SG} in Falling Film and Annular Flow Regimes.....42
Figure 4.12 Variation of Liquid Pressure Drop Multiplier against Liquid Hold-up in Falling Film Flow Regime.....44

Figure 4.13 Variation of Liquid Pressure Drop Multiplier against Liquid Hold-up in Annular Flow Regime....45
Figure 4.14 Comparison of Pressure Drop Data against Cicchitti et al. (1960) Correlation....47
Figure 4.15 Comparison of Pressure Drop Data against Lockhart-Martinelli (1949) Correlation....48
Figure 4.16 Comparison of Pressure Drop Data against Shannak (2008) Correlation....48
Figure 4.17 Comparison of Oshinowo (1971) Air-Water Pressure Drop Data against Shannak (2008) Correlation....49
Figure 4.18 Variation of Two-Phase Convective Heat Transfer Coefficient against Re_{SG} in Bubbly Flow Regime....53
Figure 4.19 Variation of Two-Phase Convective Heat Transfer Coefficient against Re_{SG} in Slug Flow Regime....54
Figure 4.20 Variation of Two-Phase Convective Heat Transfer Coefficient against Re_{SL} in Slug to Bubbly Flow Transition Regime....55
Figure 4.21 Variation of Two-Phase Convective Heat Transfer Coefficient against Re_{SG} in Froth Flow Regime....56
Figure 4.22 Variation of Two-Phase Convective Heat Transfer Coefficient against Re_{SG} in Falling Film Flow Regime....58
Figure 4.23 Variation of Two-Phase Convective Heat Transfer Coefficient against Re_{SG} in Annular Flow Regime....59
Figure 4.24 Comparison of Heat Transfer Data against Knott et al. (1959) Correlation....62
Figure 4.25 Comparison of Heat Transfer Data against Shah (1981) Correlation....63
Figure 4.26 Comparison of Heat Transfer Data against Proposed Correlation Equation (4.6)....64
Figure 4.27 Comparison of Heat Transfer Rates Upward and Downward Two-Phase Flows....66
Figure 4.28 Distribution Line for Annular Flow....69
Figure A.1 Schematic of Differential Pressure Transducer System....90

NOMENCLATURE

Symbols	Description, [unit]
A	Area, [m^2]
c_f	Fanning friction factor, [-]
c_p	Specific heat [j/K]
C	Chisholm (1967) constant, [-]
C_L	Liquid constant (Lockhart&Martinelli (1949)), [-]
C_G	Gas constant (Lockhart&Martinelli (1949)), [-]
D	Diameter, [m]
f	Darcy friction factor, [-]
F_P	Flow pattern factor (Ghajar&Tang (2007)), [-]
Fr	Froude number, $\mathrm{Fr} = \frac{G^2}{gD\rho^2}$ [-]
g	Acceleration due to gravity, [m/s^2]
G	Mass flux, [kg/m^2s]
Gr	Grashoff number (Drucker et al. (1984)), [-]
h	Convective heat transfer coefficient, [$W\ m^{-2}\ K^{-1}$]
h_z	Hydrostatic height difference, [m]
H_L	Liquid hold up, [-]
I	Current, [A]

I°	Inclination factor (Ghajar&Tang (2007)), [-]
k	thermal conductivity, [W m^{-1} K^{-1}]
L	Length, [m]
$\dot{m}$	Mass flow rate, [kg/sec]
Nu	Nusselt number, $Nu = \frac{hD}{k}$ [-]
P	Pressure, [Pa]
Pr	Prandtl number, $Pr = \frac{c_p \mu}{k}$ [-]
$\dot{q}$	Heat transfer rate, [W]
$\dot{q}''$	Heat flux, [W/m^2]
Q	Volumetric flow rate, [m^3/s]
R	Radius of pipe, [m]
r	Radial direction, [m]
r^+	Dimensionless radius, [-]
R_V	Volumetric gas to liquid ratio, U_{SG}/U_{SL} [-]
Re	Reynolds number, $Re = \frac{\rho UD}{\mu}$ [-]
R_t	Thermal resistance, [K/W]
s	Exponential parameter for Begss&Brill (1973)
T	Temperature, [ºC]
$\overline{T}$	Mean temperature, [ºC]
U	Velocity, [m/s]

V	Electrical potential difference, [V]
w	Uncertainty, [Depends on the parameter]
x	Flow quality, $\frac{\dot{m}_G}{\dot{m}_G+\dot{m}_L}$ [-]
X	Lockhart&Martinelli (1949) parameter, [-]

Greek symbols

α	Void fraction, [-]
β	Ratio parameter for homogenous model [-]
ε	Roughness, [m]
$\left[\frac{\Delta P}{\Delta L}\right]$	Pressure drop per length, [Pa/m]
λ	Volumetric ratio, $\frac{U_{SL}}{U_{SG}+U_{SL}}$[-]
μ	Dynamic viscosity, [kg/m-s]
ν	Kinematic viscosity, [m^2/s]
ρ	Density, [kg/m^3]
Φ_L	Liquid pressure drop multiplier, [-]
σ	Surface tension, [kg/s^2]
τ	Shear stress, [N/m^2]
θ	Angle of inclination, [radians]

Subscripts

atm	Atmospheric condition
b	Bulk
cal	calculated
exp	experimental
G	Gas phase
i	Inner
L	Liquid phase
M	Mixture
NS	No-slip
o	Outer
S	Slip
SG	Based on superficial gas velocity
SL	Based on superficial liquid velocity
sys	System
TP	Two-phase mixture
t	Thermal
tt	turbulent-turbulent
vv	viscous-viscous
vt	viscous-turbulent
tv	turbulent-viscous

w	Wall
wi	Inner wall
wo	Outer wall

CHAPTER I

INTRODUCTION

Two phase flow is the simultaneous flow of two different phases according to the definition in fluid mechanics. Two phase flow can be formed by either a single component or two components. Single component two phase flow generally occurs during phase change like evaporation, sublimation or condensation. On the other hand, two component flows consist of two different species which have different thermo-fluid properties. A sub category can be created depending on the phases of components. Liquid-solid, liquid-liquid, liquid-gas, and even gas-solid mixtures can be given as examples for this sub category. Due to its structure, solid phase does not have fluidity. Therefore, the flows that consist of solid components have some limitations related to the ratios of each phase since solid phase has to be carried by the other phase. On the other hand, liquid-liquid or liquid-gas flows do not have such limitations. So, various flow patterns and different characteristics can be observed for these types of flows. Beside viscosity difference, what makes liquid-gas flow even more interesting than liquid-liquid flow is the large density difference of phases. This is one of the main reasons that liquid-gas flow draws attention from the engineering community and consequently, becomes the subject of the present study like many other studies.

Another important characteristic of two-phase flow that allows us to define a different classification is the interaction of phases. Due to their chemical structures or possible surface tension between phases, we do not always expect to see a homogenous mixture. For this type of mixtures which phases do not dissolve or mix into each other under normal circumstances, there might be multiple factors like temperature, pressure or other mechanical affects that determine homogeneity or the shape and the position of each phase. This type of flow is the main area that is focused on. So, two-phase flow term is understood as liquid-gas mixture flow nowadays.

The application of two-phase flow can mainly be seen in chemical, oil and nuclear industry. Generally, systems that are used for cooling or heating are typical examples of one component two-phase flow. Air conditioner can be given as a simple example for one component two-phase flow. Since there is a phase change, higher transfer rates are expected due to latent heat transfer. This allows faster heat transportation. On the other hand, the applications of two component two-phase flow can be more seen in oil industry.

The elements that determine characteristics of liquid-gas flow are mass flow rates, thermo-fluid properties of each phase, and channel geometry. There is no doubt that another influential factor is orientation since buoyant force has the potential to make a significant effect on the flow due to the large density difference of phases. From this point of view, it can be noticed that the researchers of two phase flow generally have focused on horizontal flow; therefore, the effects of inclination on two phase flow have not been considered enough. The question arises here that what is exactly the effect of buoyant force on the flow and under which conditions it is more significant. From mechanical engineering view point, there are especially two main phenomena that we are

interested in: pressure drop and heat transfer. Void fraction and flow patterns may be considered as some assistant concepts to explain these two main phenomena. Due to complexity of two-phase flow, experimental approaches have had an importance to contribute to the topic beside theoretical approaches. So, the aim of the present work can be explained in this manner and summarized as the experimental investigation of isothermal pressure drop and non-boiling heat transfer characteristics of air-water mixture in a vertical downward orientation. By that way, we can observe what possible effects of buoyancy on two-phase pressure drop and heat transfer are when the directions of gravity force and flow are the same. In addition, we will have a chance to see the performance of some well-known two phase pressure drop and heat transfer correlations against our data. This will give us an opportunity to see possible weaknesses of correlations and to make some recommendations for future works.

The present study consists of four major chapters. Literature review and the equations of correlations that are tested against the experimental data are given in the second chapter. Chapter III is dedicated to the experimental setup, the procedure, and the explanation of some key concepts related to measurements. Chapter IV presents results and discussion of two phase pressure drop and experimental heat transfer data based on flow patterns. By showing trend of pressure drop and heat transfer rates from different perspectives, the harmoniousness of pressure drop and heat transfer (Reynolds analogy) is also discussed. In addition, performance of the correlations and a brief analysis can be found in this chapter. Lastly, conclusions drawn from this study and some recommendations for future works are summarized in chapter five.

CHAPTER II

REVIEW OF LITERATURE

2.1 Pressure Drop

In the past few decades, the application areas of two-phase flow have increased due to technological advancement. Pressure drop is especially essential in terms of engineering design whether or not the flow is isothermal. Therefore, the topic has drawn attention more and more to itself.

As explained previously, two-phase flow can be divided into several sub categories and the interest of this present study is liquid-gas flow. Another categorization can be made based on the orientation. As expected, first studies had been mostly focusing on horizontal flow. However, the large density difference between phases made studies on different orientations necessary. From this point of view, vertical orientation can be considered as the most suitable case to observe the influence of buoyancy. In spite of increasing interest on vertical flow, downward orientation has been omitted. There are dozens of studies on upward, yet the works on downward orientation in the literature are very limited.

One of the oldest works for downward two phase pressure drop is the work of Bergelin et al. (1949). Air-water combination was used as working fluid. They measured pressure drop in 0.0254 m diameter pipe. A procedure was also developed to calculate two-phase pressure drop for downward annular flow. Another attempt for downward annular flow was made by Webb and Hewitt (1975). Beside pressure drop, they also measured film thickness and liquid entrainment.

A comprehensive study for vertical two phase flow pressure drop for both upward and downward orientations was done by Oshinowo (1971). The experiment was carried out in a 0.025 m diameter pipe and air-water mixture was used as working fluid. Moreover, to see the viscosity effect, glycerol was mixed with water in specific ratios to obtain more viscous fluid phase. He observed that downward frictional pressure drop was generally higher than upward frictional pressure drop. He also observed that negative frictional pressure drop could occur for upward flow mainly in the slug-froth regime. In general, Lockhart-Martinelli (1949) correlation failed against for both upward and downward pressure drop data except for bubbly and annular regimes.

Beggs (1972) worked on two phase flow in different inclination angles to see the effect of inclination on the flow in terms of liquid hold up and pressure drop. Two different diameter sizes (0.025 m and 0.038 m) were used. Once again, fluid combination was air-water mixture. Beggs (1972) observed that liquid hold up was greatly influenced by inclination angle and at the same time, pressure drop was influenced by liquid hold up. Based on his observations, he defined three flow regimes and developed different liquid hold up correlations for each of flow regimes. He also developed a friction factor correlation that was independent of flow regime but dependent on liquid hold up.

Yamazaki&Yamaguchi (1979) studied downward two phase flow for air-water system in 0.025 m diameter pipe to observe the characteristics of flow pattern, liquid hold up and pressure drop of the flow. They also developed correlations for liquid hold up and pressure drop.

Mukharjee (1979) investigated two phase flow for different inclination angles. Air-kerosene and air-oil were used as working fluids in 0.038 m diameter pipe. Different correlations were developed for liquid hold up and pressure drop depending on flow regime and inclination.

Annular downward two phase pressure drop was studied experimentally by Hajiloo et al. (2001). Four different tubes (ranging from 0.0156 – 0.0412 m) were used to see the effect of pipe diameter. They found that existing correlations were unsuccessful against their data. A dimensionless film thickness was defined and an empirical correlation was developed to predict annular pressure drop.

Since we do not have enough correlations those are specifically developed for downward orientation, it would be more meaningful to check correlations in terms of frictional pressure drop in order to be able to use some other well-known correlations that were developed for horizontal and upward orientations. Beside some empirical or graphical approaches, we can mainly classify two-phase pressure drop correlations as homogenous and separated flow models. The pressure drop correlations based on homogenous and separated flow models are given in Table 2.1 and Table 2.2, respectively.

Table 2.1 Homogenous Pressure Drop Correlations

Homogenous Model **Two-Phase Pressure Drop Correlations**	
Beattie&Whalley (1982)	$\mu_{TP} = \beta\mu_G + (1-\beta)(1+2.5\beta)\mu_L$ $\beta = \frac{\rho_L x}{\rho_L x + \rho_G(1-x)}$
Cicchitti et al. (1960)	$\mu_{TP} = x\mu_G + (1-x)\mu_L$
Dukler et al. (1964)	$\mu_{TP} = \beta\mu_G + (1-\beta)\mu_L$ $\beta = \frac{\rho_L x}{\rho_L x + \rho_G(1-x)}$
McAdams et al.(1942)	$\mu_{TP} = [\frac{x}{\mu_G} + \frac{1-x}{\mu_L}]^{-1}$
Shannak (2008)	$Re_{TP} = \frac{x^2 + (1-x)^2\,(\rho_G/\rho_L)}{\frac{x^2}{Re_{SG}} + \frac{(1-x)^2}{Re_{SL}}\frac{\rho_G}{\rho_L}}$ $Re_{TP} \geq 11\ then$ $\frac{1}{f_{TP}{}^{1/2}} = -2Log10[\frac{\varepsilon/D}{3.7065} - \frac{5.0452}{Re_{TP}}Log10\left(\frac{(\varepsilon/D)^{1.1098}}{2.8257} + \frac{5.8506}{Re_{TP}{}^{0.8981}}\right)]$ $Re_{TP} < 11\ then$ $f_{TP} = \frac{64}{Re_{TP}}$

Beggs&Brill (1973)	$\mu_{TP} = (1-\lambda)\mu_G + \lambda\mu_L$ $f_{NS} = [4Log10(\frac{Re_{TP}}{4.5223Log10(Re_{TP}) - 3.8215})]^{-2}$ $\frac{f_{TP}}{f_{NS}} = e^s$ $y = \frac{\lambda}{(1-\alpha)^2}$ $1 < y < 1.2\ then$ $s = \ln(2.2y - 1.2)$ $y < 1\ or\ y > 1.2\ then$ $s = [\frac{\ln(y)}{-0.0523 + 3.182\ln(y) - 0.8725\ln(y)^2 + 0.01853\ln(y)^4}]$

Some Definitions and Explanations

$U_{SL} = \frac{\dot{m}_L}{\rho_L A}$

$U_{SG} = \frac{\dot{m}_G}{\rho_G A}$

$\lambda = \frac{U_{SL}}{U_{SL} + U_{SG}}$

$U_M = U_{SL} + U_{SG}$

$x = \frac{\dot{m}_G}{\dot{m}_L + \dot{m}_G}$

$\rho_{TP} = [\frac{x}{\rho_G} + \frac{1-x}{\rho_L}]^{-1}$

$Re_{SL} = \frac{\rho_L U_{SL} D}{\mu_L}$

$Re_{SG} = \frac{\rho_G U_{SG} D}{\mu_G}$

$Re_{TP} = \frac{\rho_{TP} U_M D}{\mu_{TP}}$ #

$\frac{1}{{c_{f_{TP}}}^{1/2}} = 3.48 - 4\, Log10(\frac{2\,\varepsilon}{D} + \frac{9.35}{Re_{TP}\, {c_{f_{TP}}}^{\frac{1}{2}}})$ #

$\frac{\Delta P_{TP}}{\Delta L} = \frac{2\, c_{f_{TP}}}{D}\, \rho_{TP} U_M^2$ *

- # For all correlations except Shannak (2008) and Beggs&Brill (1973)
- $*c_{f_{TP}} = \frac{f_{TP}}{4}$

Table 2.2 Separated Flow Pressure Drop Correlations

Separated Flow Model **Two-Phase Pressure Drop Correlations**	
Lockhart&Martinelli (1949)	$X_{vv}^2 = \frac{\dot{m}_L}{\dot{m}_G}\frac{\rho_G}{\rho_L}\frac{\mu_L}{\mu_G}$ $X_{vt}^2 = Re_{SG}^{-0.8}\frac{C_L}{C_G}\frac{\dot{m}_L}{\dot{m}_G}\frac{\rho_G}{\rho_L}\frac{\mu_L}{\mu_G}$ $X_{tv}^2 = Re_{SL}^{0.8}\frac{C_L}{C_G}\frac{\dot{m}_L}{\dot{m}_G}\frac{\rho_G}{\rho_L}\frac{\mu_L}{\mu_G}$ $X_{tt}^2 = \frac{\dot{m}_L}{\dot{m}_G}(\frac{\rho_G}{\rho_L})^{0.555}(\frac{\mu_L}{\mu_G})^{0.111}$ $C_L = C_G = 0.046$ Viscous-viscous $C_L = 16, C_G = 0.046$ Turbulent-viscous $C_L = 0.046, C_G = 16$ Viscous-turbulent

	$C_L = C_G = 16$ Turbulent-turbulent
Chisholm (1967)	$\Phi_L^2 = 1 + \frac{C}{X} + \frac{1}{X^2}$ $C = 5$ Viscous-viscous $C = 10$ Turbulent-viscous $C = 12$ Viscous-turbulent $C = 20$ Turbulent-turbulent
Sun&Mishima (2009)	$\Phi_L^2 = 1 + \frac{C_{sm}}{X^{1.19}} + \frac{1}{X^2}$ $C_{sm} = 1.79[\frac{Re_{SG}}{Re_{SL}}]^{0.4}(\frac{1-x}{x})^{1/2}$

Some Definitions and Explanations

$$\left[\frac{\Delta P}{\Delta L}\right]_{TP} = \Phi_L^2 \left[\frac{\Delta P}{\Delta L}\right]_L$$

- $\left[\frac{\Delta P}{\Delta L}\right]_L$ is superficial single phase liquid pressure drop. It can be calculated by using a suitable correlation or Moody Chart.
- To find Φ_L^2 for Lockhart&Martinelli (1949), original paper has to be used since the relation between Φ_L and X was represented graphically. More information can be found in the study. Chisholm (1967) provides an approximate solution to avoid the graphic.
- C_L and C_G values are needed to calculate X values that is used by all the correlations based on the separated model. Determination of these values depends on the transition from the laminar to turbulent that is not certain. However Re≈2000 can be accepted. The other C values that are used to calculate liquid

pressure drop multiplier (Φ_L^2) should also be determined by the criteria given above unless it is given as a function of Re itself.

2.2 Heat Transfer

As mentioned earlier, two-phase heat transfer can be classified depending on whether or not phase change occurs. The term itself is generally understood as boiling heat transfer. Therefore, it is more suitable to express two components two phase flow heat transfer as non-boiling two-phase heat transfer.

The studies on non-boiling two-phase heat transfer in downward orientation are even more limited than the pressure drop's. There are three important studies that can be found in the literature: Dorresteijn (1970), Chu&Jones (1980), Oshinowo et al. (1984). In all three, heat transfer measurements were done for both upward and downward orientations. Air-water was used as working fluid for Chu&Jones (1980) and Oshinowo et al. (1984), whereas air-oil was employed in Dorresteijn (1970). All three studies have an agreement that upward heat transfer coefficient is generally higher than downward heat transfer coefficient for the same liquid-gas flow rates if liquid phase is in laminar or transition region. According to Chu&Jones (1980), downward heat transfer coefficient can be higher in fully turbulent region. Oshinowo et al.(1984) also reported that the heat transfer difference between upward and downward orientation generally increased with decreasing liquid flow rate.

The heat transfer correlations tested against our data are given in Table 2.3

Table 2.3 Two-phase Flow Heat Transfer Correlations

Aggour (1978)	$\frac{h_{TP}}{h_L} = (1-\alpha)^{-1/3}$ Laminar Where $Nu_L = 1.615\,(\frac{Re_{SL}Pr_L D}{L})^{1/3}(\mu_B/\mu_W)^{0.14}$ $\frac{h_{TP}}{h_L} = (1-\alpha)^{-0.83}$ Turbulent Where $Nu_L = 0.0155\,{Re_{SL}}^{0.83}Pr_L^{0.5}(\mu_B/\mu_W)^{0.33}$
Chu&jones (1980)	$Nu_{TP} = 0.43Re_{TP}^{0.55}Pr_L^{1/3}(\mu_B/\mu_W)^{0.14}(P_{atm}/P_{sys})^{0.17}$ Where $Re_{TP} = Re_{SL}/(1-\alpha)$
Dorresteijn (1970)	$\frac{h_{TP}}{h_L} = (1-\alpha)^{-1/3}$ Laminar $\frac{h_{TP}}{h_L} = (1-\alpha)^{-0.8}$ Turbulent Where $Nu_L = 0.0123\,{Re_{SL}}^{0.9}Pr_L^{0.33}(\mu_B/\mu_W)^{0.4}$
Drucker et al. (1984)	$\frac{h_{TP}}{h_L} = 1 + 2.5(\alpha\, Gr/Re_{TP}^2)^{0.5}$ $Gr = [(\rho_L - \rho_G)gD^3]/(\rho_L {\nu_L}^2)$
Katsuhara&Kazama (1958)	$Nu_{TP} = 8.7(1-\alpha)^{0.125}Re_{TP}^{0.25}Pr_{TP}^{0.4}$ $\rho_{Tp} = \alpha\rho_G + (1-\alpha)\rho_L$ $k_{TP} = \alpha\frac{\rho_G}{\rho_{Tp}}k_G + (1-\alpha)\frac{\rho_L}{\rho_{Tp}}k_L$ $Pr_{TP} = \alpha\frac{\rho_G}{\rho_{Tp}}Pr_G + (1-\alpha)\frac{\rho_L}{\rho_{Tp}}Pr_L$ $U_{TP} = \dot{m}_{Total}/(\rho_{Tp}\,\pi\,D^2/4)$ $\nu_{TP} = \alpha\frac{\rho_G}{\rho_{Tp}}\nu_G + (1-\alpha)\frac{\rho_L}{\rho_{Tp}}\nu_L$ $Re_{TP} = \frac{U_{TP}D}{\nu_{TP}}$ $h_{TP} = Nu_{TP}k_{TP}/D$
Khoze et al. (1976)	$Nu_{TP} = 0.26Re_{SG}^{0.2}Re_{SL}^{0.55}Pr_L^{0.4}$
Knott et al. (1959)	$\frac{h_{TP}}{h_L} = (1+\frac{U_{SG}}{U_{SL}})^{1/3}$ Where h_L is from Seider&Tate (1936)
Kudirka et al. (1965)	$Nu_{TP} = 125(\frac{U_{SG}}{U_{SL}})^{1/8}(\mu_G/\mu_L)^{0.6}\,Re_{SL}^{1/4}Pr_L^{1/3}(\mu_B/\mu_W)^{0.14}$
Kim et al. (2000)	$\frac{h_{TP}}{h_L} = (1-\alpha)\{1 + 0.27[(\frac{x}{1-x})^{-0.04}(\frac{\alpha}{1-\alpha})^{1.21}(\frac{Pr_G}{Pr_L})^{0.66}(\frac{\mu_G}{\mu_L})^{-0.72}]\}$ Where h_L is from Seider&Tate (1936)
Oshinowo et al. (1984)	$Nu_{TP} = 1.2{R_V}^{0.1}(\mu_G/\mu_L)^{0.2}\,Re_{SL}^{0.6}Pr_L^{1/3}(\mu_B/\mu_W)^{0.14}$ Where $R_V = (U_{SG}/U_{SL})$
Ravupudi&Godbold (1978)	$Nu_{TP} = 0.56(\frac{U_{SG}}{U_{SL}})^{0.3}(\mu_G/\mu_L)^{0.2}\,Re_{SL}^{0.6}Pr_L^{1/3}(\mu_B/\mu_W)^{0.14}$
Shah (1981)	$\frac{h_{TP}}{h_L} = (1+\frac{U_{SG}}{U_{SL}})^{1/4}$ $Nu_L = 1.86\,(\frac{Re_{SL}Pr_L D}{L})^{1/3}(\mu_B/\mu_W)^{0.14}$ Laminar $Nu_L = 0.023\,{Re_{SL}}^{0.8}Pr_L^{0.4}(\mu_B/\mu_W)^{0.14}$ Turbulent

Tang&Ghajar (2007)	$\frac{h_{TP}}{h_L} = F_P\{1 + 0.55[(\frac{x}{1-x})^{0.1}(\frac{1-F_P}{F_P})^{0.4}(\frac{Pr_G}{Pr_L})^{0.25}(\frac{\mu_L}{\mu_G})^{0.25} I^{0.25}]\}$ $F_P = (1-\alpha) + \alpha[\frac{2}{\pi} tan^{-1}\{(\frac{\rho_G(U_G-U_L)^2}{gD(\rho_L-\rho_G)})^{\frac{1}{2}}\}]^2$ $I^{\circ} = 1 + \left[\left(\rho_L - \rho_G\right) gD^2 \lvert sin\theta \rvert\right]/\sigma$ Where h_L is from Seider&Tate (1936)
Tang&Ghajar (2011)	$\frac{h_{TP}}{h_L} = F_P^{1/2} \frac{\dot{m}_L}{\dot{m}_{Total}} (\frac{\rho_L}{\rho_{TP}})^{1/2} \Phi_L^{1/5}$ $F_P = (1-\alpha) + \alpha[\frac{2}{\pi} tan^{-1}\{(\frac{\rho_G(U_G-U_L)^2}{gD(\rho_L-\rho_G)})^{\frac{1}{2}}\}]^2$ $\rho_{Tp} = \alpha\rho_G + (1-\alpha)\rho_L$ $\Phi_L = (\frac{\Delta P_{TP}}{\Delta P_L})^{0.5}$ Where h_L is from Seider&Tate (1936)
Ueda&Hanaoka (1967)	$Nu_{TP} = \frac{0.075 Re_M^{0.6} Pr_L}{1 + 0.035(Pr_L - 1)}$ $U_S = U_G - U_L$ $Re_S = \frac{U_S D(1-\alpha^{0.5})}{\nu_L}$ $U_{ED} = U_{SL} + U_{SG}$ $Fr_{ED} = g\alpha D(1-\alpha^{0.5})/U_{ED}^2$ $Fr_S = g\alpha D(1-\alpha^{0.5})/U_S^2$ $U_M = U_L + 1.2 {Re_S}^{-0.25} U_S - 12 Fr_{ED} U_{ED} + 16 {Fr_S}^{1.25} U_S$ $Re_M = \frac{U_M D}{\nu_L}$
Vijay et al. (1982)	$\frac{h_{TP}}{h_L} = (\frac{\Delta P_{TP}}{\Delta P_L})^{0.451}$ Where h_L is from Seider&Tate

- Re_{SL} <2000 Laminar except Shah (1981) Correlation. Re_{SL} < 170 for Shah (1981).
- When using Seider&Tate (1936) correlation for Kim et al. (2000) and Tang&Ghajar (2007) correlations, use situ Reynolds number $Re_{situ} = \frac{4\dot{m}_L}{\pi(1-\alpha)^{0.5}\mu_L D}$
- $h_{TP} = Nu_{TP} k_L/D$ for Nu_{TP} type correlations except Katsuhara&Kazama (1958)
- Please notice that Tang&Ghajar (2011) and Vijay et al. (1982) are Reynolds analogy correlations. Therefore, pressure drop multiplier must be known.

CHAPTER III

EXPERIMENTAL SETUP

In this chapter, the experimental setup and its instruments are explained briefly. In addition, the procedure to measure two phase frictional pressure drop and heat transfer coefficient is discussed. An overall system diagram is given in Figure 3.1.

The experimental setup which was designed by Wendell Cook (2008) allows experimenters to perform flow visualization, void fraction, pressure drop, and heat transfer measurements. There are two separate test branches for different purposes. The flow visualization and the void fraction measurements can be conducted in the flow visualization/void fraction section whereas the pressure drop and the heat transfer measurements can be performed in the heated section. Since the subject of this study is two phase pressure drop and heat transfer in vertical downward orientation, only heated section and its components will be described.

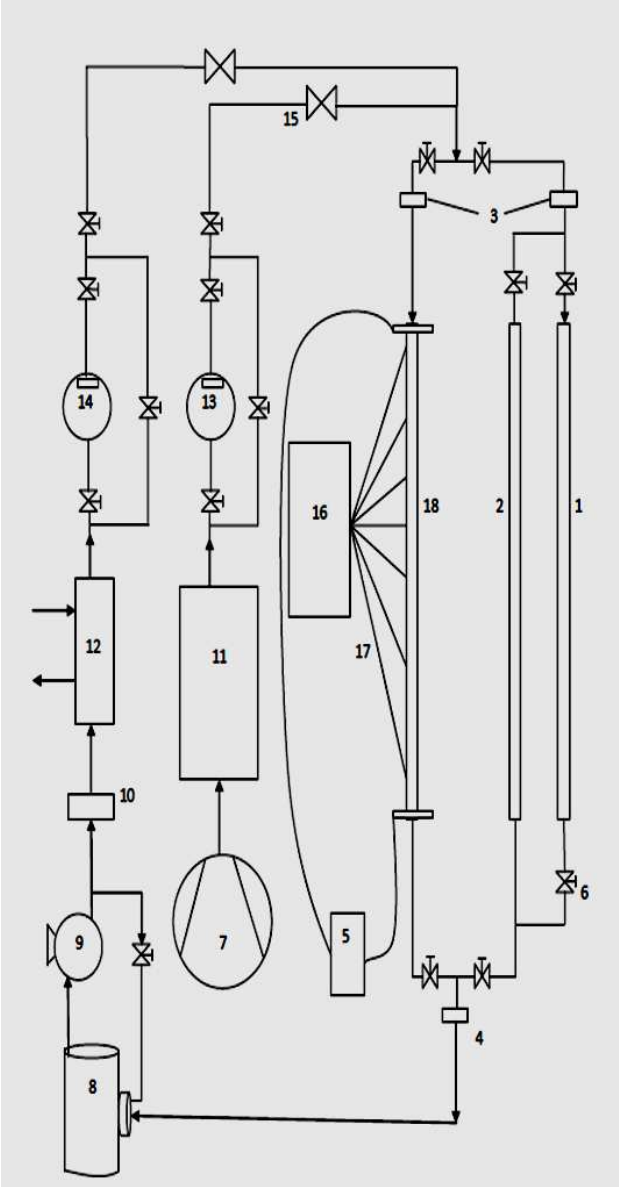

1. Flow visualization/void fraction section
2. By pass line
3. Inlet thermocouple probe
4. Outlet thermocouple probe
5. D.C. Arc welder
6. Solenoid Valves
7. Air Compressor
8. Water Tank (55 Gal)
9. Centrifugal Pump
10. Water Filter
11. Air Side Heat Exchanger
12. Water Side Heat Exchanger
13. Coriolis Gas Flow Meter
14. Coriolis Liquid Flow Meter
15. Check Valves at Inlet
16. National Instruments Board and CPU
17. Thermocouples
18. Heated Section

Figure 3.1 Schematic of Experimental Setup

3.1 Details of Experimental Setup

A photograph of the test branches is given in Figure 3.2. The insulated section which is seen on the right side in the photo is the heated section. Three major components of the heated section are mixing sections, a heated section and a thermocouple array.

Mixing Section: Two different mixing sections are placed in the heated section in order to help mixing. One mixer is placed at the inlet and the second one is placed at the outlet. This will lead to better accuracy to measure the temperature of the mixture. Both mixers used in the setup are Koflo model 3-8 40-C-4-3V-2.

Heated Section: A schematic of the heated section is given in Figure 3.3. 3/8 inch nominal schedule 40 IPS alloy stainless steel was used in the heated section. That provides an actual inner diameter of 1.252 cm. The length of the test section is 101.6 cm. A Miller Maxtron 450 model arc welder was used to heat the test section via high current passing through the pipe. Copper plates were attached to both sides of the pipe as conductive connections by silver soldering. For insulation purpose, phenolic resin boards are used in order to reduce heat loss from the heated section. Moreover, Micro-Lok Fiber Glass Pipe insulation produced by Johns Manville and Thermwell Fiber-Glass Pipe Insulation wrap are other insulation materials used in the heated section.

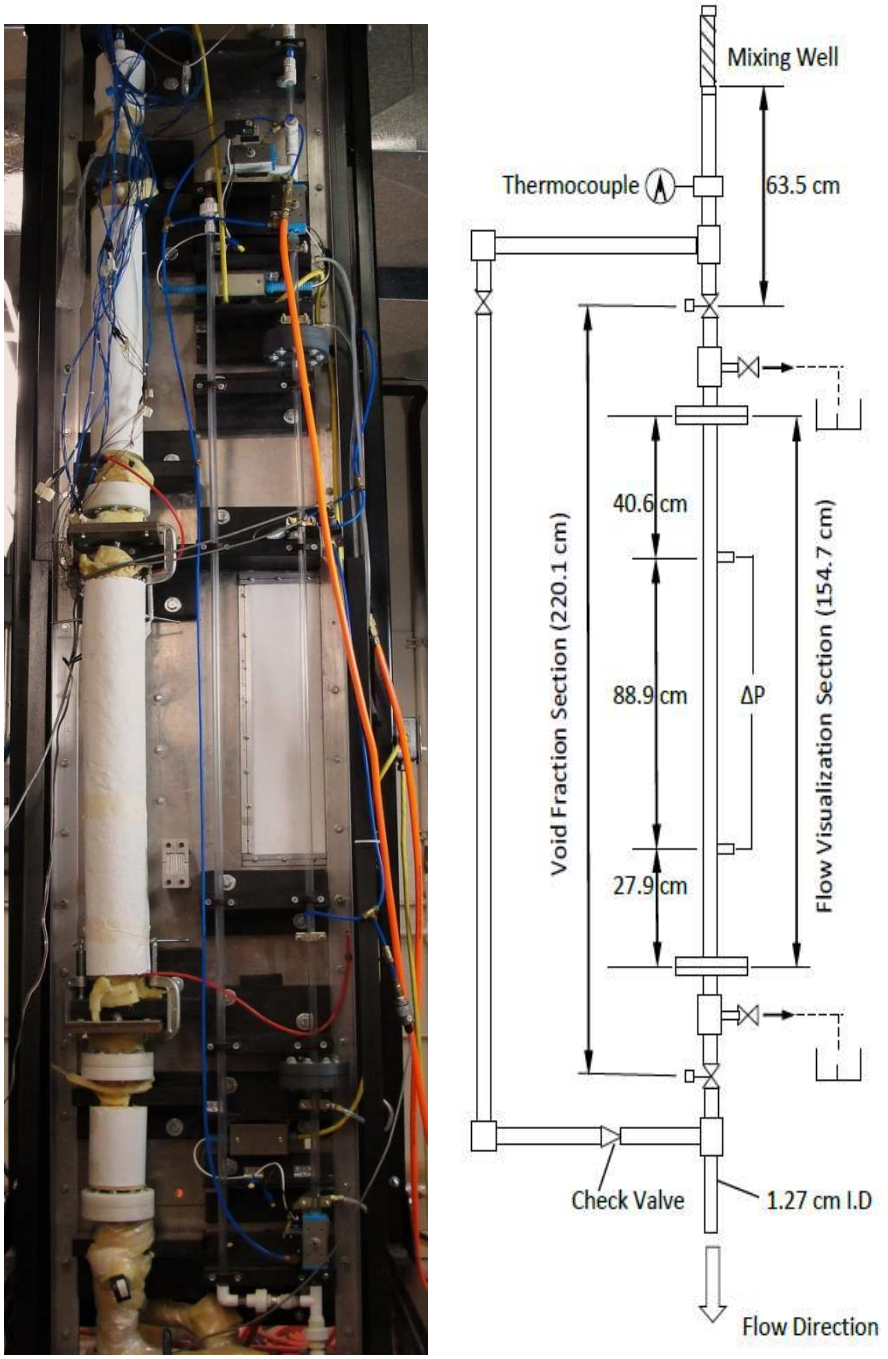

Figure 3.2 Photograph of Experimental Setup and Schematic of Flow Visualization and Void Fraction Sections

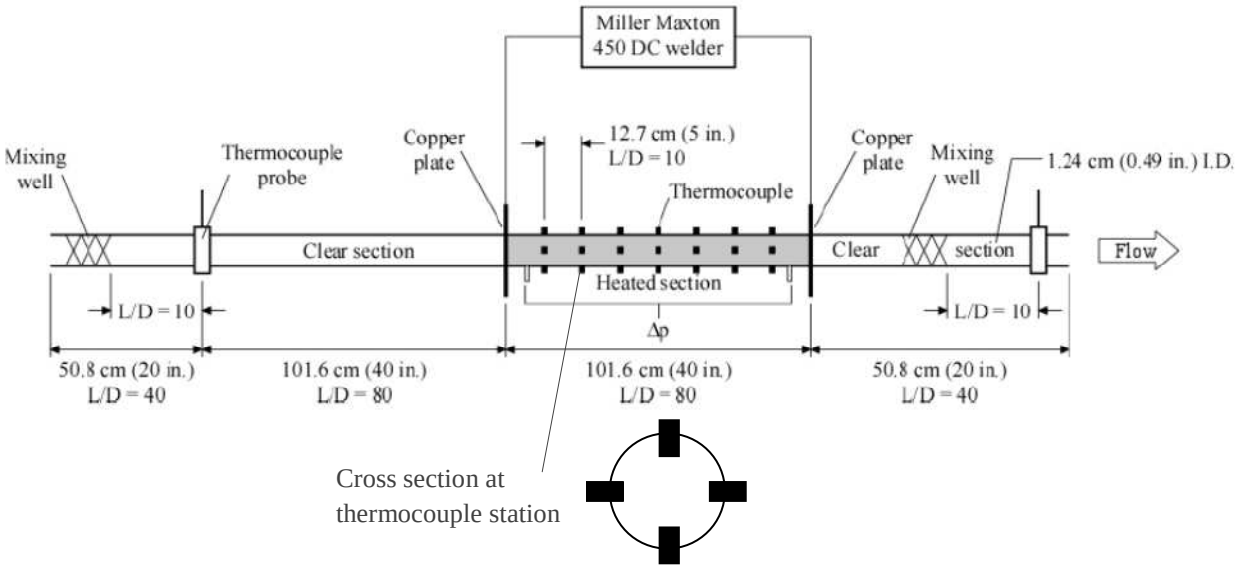

Figure 3.3 Schematic of Heated Section

A Validyne model DP-15 pressure transducer with a CD15 carrier demodulator was used for the two phase pressure drop measurements. Beside its high accuracy, the model also allows different diaphragms for different pressure drop ranges. In the present study, 2 psi diaphragm was sufficient for most of the runs. When pressure exceeded 2 psi, for some experiments, a 5 psi diaphragm was used. Although the heated section is capable to perform isothermal pressure drop measurements, only non-isothermal pressure drop were measured in this work. The accuracy associated with the pressure drop diaphragm is ±0.25% of full scale.

Thermocouple Array: There are two thermocouple probes placed at the inlet and outlet of the test section. In addition, there are seven thermocouple stations employed along the pipe to measure outer wall temperature of the pipe. Each thermocouple station consists of four thermocouples in order to increase accuracy. As seen in Figure 3.3, cross section

diagram, wall thermocouples are placed with π/4 radian intervals. All thermocouples used in the setup are Omega Model TMQSS—06U—6 and have an accuracy of ±1.0 ℃.

Water Circulation System: Purified water is used as working liquid in the experimental setup. A 55 gal cylindrical tank is used for storage. The water is pumped into the system via a Bell and Gosset series 1535 coupled centrifugal pump (model number 3445 D10) as seen in Figure 3.4. Then, the water passes through an Aqua-Pure AP12T purifier. Later, the water arrives to an ITT standard model BCF 4063 one shell and two tube pass heat exchanger. After leaving from the heat exchanger, it passes through the flow meter. The flow rate is measured by Emerson (Micro Motion Elite Series model number CMF 100) Coriolis mass flow meter. The water mixes with the air in the mixing section and comes to the test section afterwards. Finally, it returns to the water tank.

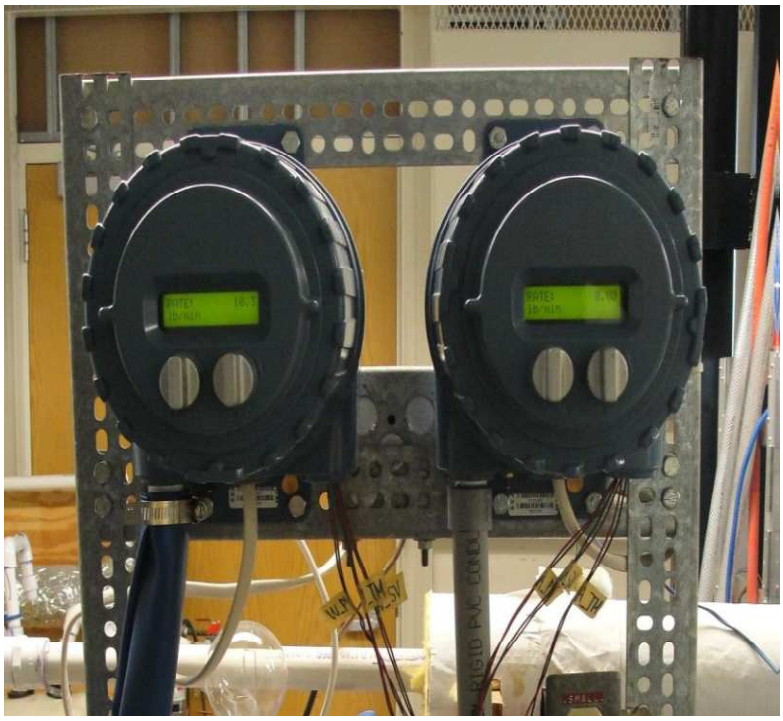

Figure 3.4 Water Mass Flow Meters

Air Circulation System: The compressed air is introduced into the system by Ingersoll-Rand T30 Model 2545 air compressor as seen in Figure 3.5. Next step is a regulator/ filter component. Then, the air arrives to a coil submerged heat exchanger. After leaving from the coil, it is filtered again. Air flow rate is regulated by a Parker Model 24NS 82(A)-V8LN-SS Needle Valve before it passes through Emerson Flow Meters (Micro Motion Elite Series Model number LMF 3M and CMF025). There are two flow meters for the air system. Either of flow meters can be used depending on the air flow rate range which is worked on. As similar to the water system, the air comes to the mixing section, then to the test section and, finally returns to the tank.

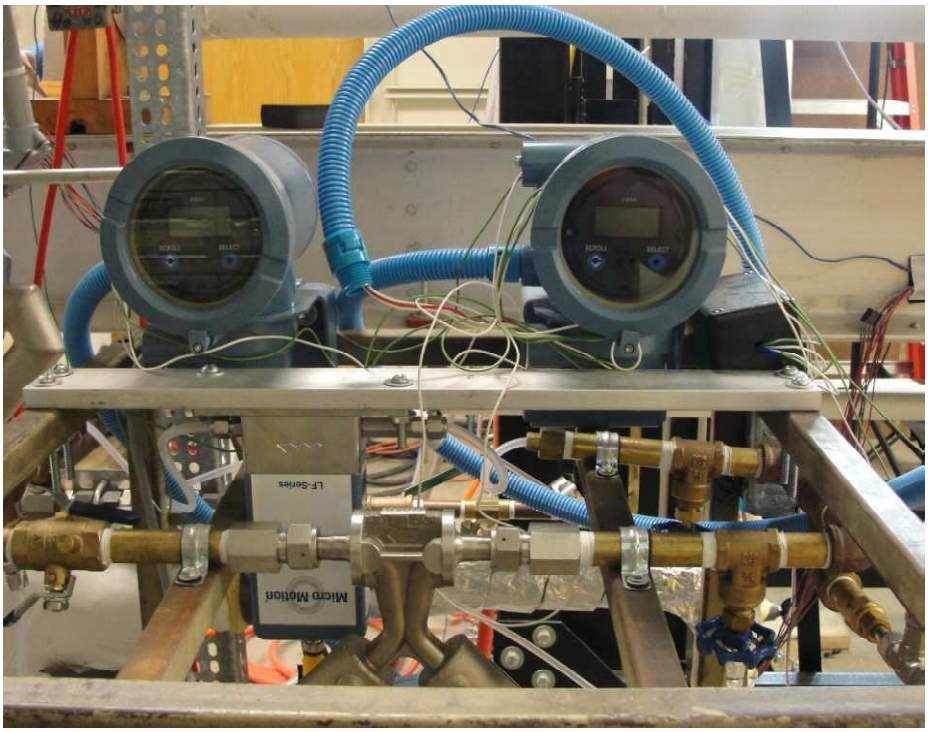

Figure 3.5 Air Mass Flow Meters

3.2 Data Acquisition System

A data acquisition system by National Instruments is used to record the data. The flow rates of each phase, the temperatures of the entry, exit and the thermocouples in the each station, system pressure, pressure drop, voltage and ampere can be monitored and recorded via the system. There are three basic elements in the system: chassis, module, and terminal blocks. Wendell Cook's work (2008) can be referred to for more information about these elements. LabVIEW by National Instruments is used as a graphical interface program. A former Ph.D. student Jae-Yong Kim wrote a data acquisition for a previous setup. Necessary modifications were made by another former Ph.D. student Clement Tang for the current setup.

3.3 Experimental Procedure

3.3.1 Pressure Drop Measurements

A detailed procedure for pressure drop measurements is given in Cook (2008). As a summary, we can reduce the procedure into five steps: pre-operation checks, system warm up, stabilization, recording, and shut down.

Beside the basic steps mentioned above, there are several important points that should be considered before conducting two phase pressure drop experiments. The first one is to select a suitable diaphragm for the desired flow ranges. This may require a large diaphragm to determine an approximate pressure drop range before starting actual readings. Once the pressure drop range is determined, then smaller diaphragms can be used in order to increase accuracy.

Another important issue is to how to measure two phase frictional pressure drop in vertical orientation. A pressure drop balance can be written as follows:

$$\Delta P_{Total} = \Delta P_{Hydrostatic} + \Delta P_{Frictional} + \Delta P_{Acceleration} \quad (3.1)$$

The acceleration pressure drop can be neglected for the measurement in short pipes due to the very small void fraction changes along the pipe. Then, the equation for frictional pressure drop becomes:

$$\Delta P_{Frictional} = \Delta P_{Total} - \Delta P_{Hydrostatic} \quad (3.2)$$

Now, the hydrostatic pressure drop can be defined based on mixture density.

$$\Delta P_{Hydrostatic} = -g\ \rho_{TP}\ h_z \quad (3.3)$$

Where mixture density is defined as follows:

$$\rho_{TP} = \alpha\rho_G + (1-\alpha)\rho_L \quad (3.4)$$

Then, the frictional pressure drop can be written as follows:

$$\Delta P_{Frictional} = \Delta P_{Total} + g\ h_z\ [\alpha\rho_G + (1-\alpha)\rho_L] \quad (3.5)$$

Consequently, frictional pressure drop can be calculated after measuring total pressure drop. The vertical pressure drop measurement can be done in two ways. The first one is simply to use two manometers (Figure 3.6). In this situation, total pressure drop is equal to the measured pressure drop since total pressure is measured by subtraction of the pressure at point 1 from the pressure at point 2.

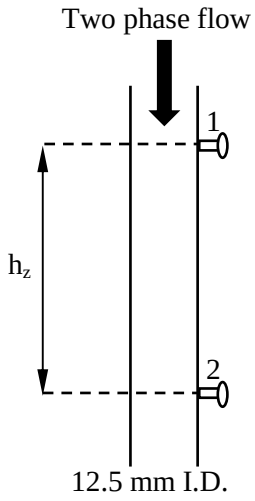

Figure 3.6 Schematic of Two Manometers System

The second way is to use a differential pressure transducer (Figure 3.7). As it can be seen, the measured pressure drop is different than the measured pressure drop in the first system. If the pipes attached to pressure transducer are filled up with the liquid, then it can be shown that:

$$P_A = P_1 + g\ h_1\ \rho_L \tag{3.6}$$

$$P_B = P_2 - g\ h_2\ \rho_L \tag{3.7}$$

Then, the relation between the total pressure drop and the measured pressure drop becomes:

$$\Delta P_{12} = \Delta P_{AB} - g\ (h_1 + h_2)\ \rho_L = \Delta P_{AB} - g\ h_z\ \rho_L \tag{3.8}$$

Now, if we put the equation (3.8) into the equation (3.5), we will get:

$$\Delta P_{Frictional} = \Delta P_{AB} - g\ h_z\ \rho_L + g\ h_z\ [\alpha\rho_G + (1-\alpha)\rho_L] \tag{3.9}$$

If we simplify, we will get:

$$\Delta P_{Frictional} = \Delta P_{AB} + g\ h_z\ \alpha(\rho_G - \rho_L) \tag{3.10}$$

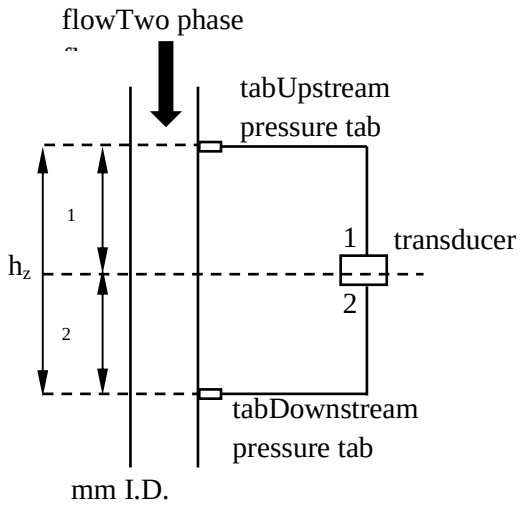

Figure 3.7 Schematic of Differential Pressure Transducer System

Please, notice that the measured pressure drop is equal to frictional pressure drop for single phase flow for the system shown in Figure 3.7 since the void fraction is zero. This can also be easily understood that there is no height difference between point A and point B. As a result, there will not be a hydrostatic pressure difference between point A and point B. So, the difference between the two systems is what the measured pressure drop corresponds to. Using a differential pressure transducer is probably more suitable for short pipes since it is more accurate. However, the pipes attached to the transducer should be monitored carefully. Especially for high system pressure, air can slip into these pipes and can significantly change results since the equation (3.8) is based on the assumption that transducer's pipes are filled up with only liquid. Otherwise, the void fractions in the transducer's pipes have to be known whereas that is not practical. The

two manometers system is more suitable for longer pipes which do not require much sensitivity due to the high pressure drop and it does not need any special attention unlike the differential pressure transducer system.

3.3.2 Heat Transfer Measurements

A detailed procedure for heat transfer measurements is given again in Cook (2008). The procedure is similar to the pressure drop measurement; however, it needs more attention. Beside some safety reasons due to the usage of the welder, stabilization is another difficulty for two phase heat transfer runs and can take longer time depending on the flow ranges of each phase, the temperature of the air and the tap water. It is wise to open heat exchanger's valve and let the system become cooler and stabilize before turning on the welder. This will significantly reduce the time needed for stabilization. Otherwise, it will probably take much time.

Another important point is the flow ranges which are being worked on. Some flow patterns like slug, falling film are more chaotic and may require more time for both stabilization and data recording. Moreover, there may be some limitations due to the safety issues or accuracy, repeatability and reliability of the data. It is more likely to face these kinds of problems especially in very low liquid flow rates and/or very high gas flow rates. For instance, one can expect high heat balance error and uncertainty in such flow rates. Falling film and annular film are good examples of these types of patterns that can cause an increase in the uncertainty. One way to overcome the problem is to increase heat given by the welder. This may significantly decrease uncertainty, however; the system must be monitored against overheating that can not only cause dry spots but also harm the experimental setup.

Consequently, some flow rate ranges may require pre-work. By that way, an idea can be had about the behavior of the flow. This can provide important clues about optimum stabilization and recording time, and limitations of the heat transfer measurements of the desired flow rates which are being worked on. Some general observations and recommendations based on the present study about the flow pattern are given in Table 3.1.

Table 3.1 Recommendations for Two-phase Heat Transfer Measurements

Flow Pattern	**Recommended Data Recording Time**	**Flow/Heat Transfer Characteristics**	**Possible Uncertainty**
Annular	3-5 minutes	Stable	High
Bubble	3 minutes	Stable	Low
Falling Film	5-10 minutes	Unstable, Dry Spots	High
Froth	5 minutes	Stable/Low Fluctuations	Moderate
Slug	5-10 minutes	Unstable/High Fluctuations	Low

3.4 Data Acquisition

The main function of data reduction program is to calculate inner wall temperature and heat flux by using a finite difference formulation, since it is difficult to measure inside wall temperature. The program was developed by Jae-Yong Kim (former PhD student) and was based on the idea of Ghajar and Zurigat (1991). Later, it was modified by Clement Tang (former PhD student) for the present setup. More information about the data reduction program can be found in Ghajar and Kim (2006).

3.5 Validation of Experimental Setup

Before conducting two phase flow pressure drop and heat transfer runs, it was necessary to be sure that the experimental setup was working properly. For this purpose, single phase pressure drop and heat transfer measurements were performed and compared against some well-known correlations. The uncertainty analysis can be found in Appendix A.

3.5.1 Single Phase Pressure Drop Measurements

Distilled water was used to conduct the single phase pressure drop measurements to check whether or not the experimental setup is working properly in vertical orientation. The Darcy friction factor concept is used for comparison.

$$f = \frac{2D\Delta P}{\rho L V^2} = \frac{\Delta P D^5 \pi^2 \rho}{8L^2} \tag{3.11}$$

In this formula, ΔP and $\dot{m}$ are obtained by the Validyne pressure transducer and Coriolis Flow meter, respectively. Pipe diameter (D) and length (L) were measured. Linstrom and Mallard (2003) equation was used to obtain water density (ρ).

$$\rho = 999.96 + 1.7158 \times 10^{-2} T - 5.8699 \times 10^{-3} T^2 + 1.5487 \times 10^{-5} T^3 \tag{3.12}$$

Here temperature and density are in ℃ and kg/m^3, respectively. The Colebrook-White (1939) equation is preferred since it is considered as one of the most accurate and robust correlations for pressure drop in pipes.

$$\frac{1}{\sqrt{f}} = -2log_{10}\left(\frac{\varepsilon}{3.7D} + \frac{2.51}{Re\sqrt{f}}\right) \tag{3.13}$$

Here ε=0.0000152 m is taken. Figure 3.8 shows the experimental results versus the Colebrook-White (1939) equation for 9000 < Re < 38000. The measurements were obtained by using a 2 psi diaphram. It is better to avoid to get data for points close to diaphrams' upper and lower limits. For this purpose, the points were within 0.2 psi - 1.8 psi pressure drop range.

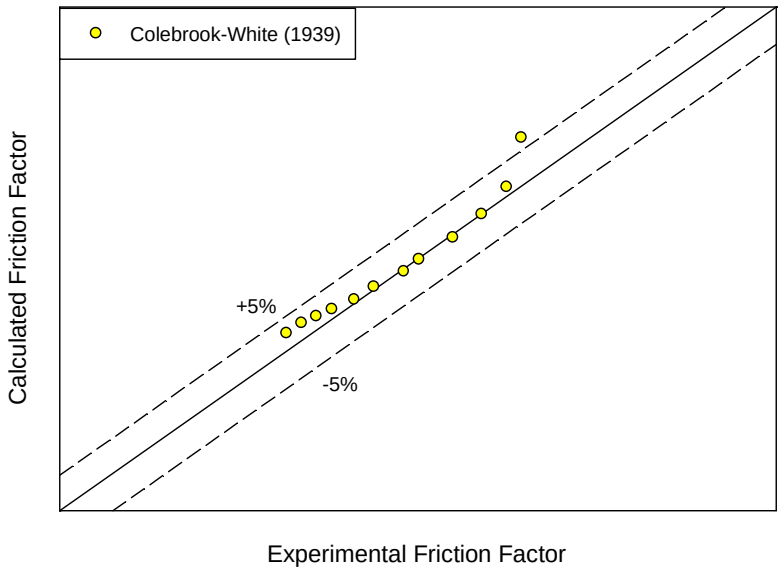

Figure 3.8 Single Phase Pressure Drop Measurements against Colebrook-White Equation

The overall error of the single phase runs against Colebrook-White (1939) equation was almost within ±5%. This shows the experimental setup produces quite reasonable results.

3.5.2 Single Phase Heat Transfer Measurements

The single phase data was collected for 9000 < Re < 25000 and compared against five heat transfer correlations for comparison. The selected correlations were Dittus and Boelter (1930), Chilton and Colburn (1934), Seider and Tate (1936), Gnielinski (1976),

and Ghajar ana Tam (1994). The correlations and their limitations are given in the Table 3.2.

Table 3.2 Single Phase Heat Transfer Correlations

Dittus&Boelter (1930)	$Nu_D = 0.023 Re_D^{4/5} Pr^n$ where n = 0.4 for heating	$0.7 \leq Pr \leq 160$ $Re_D \geq 10000$ $L/D \geq 10$
Seider&Tate (1936)	$Nu_D = 0.023 Re_D^{0.8} Pr^{1/3} (\mu_b/\mu_w)^{0.14}$	$0.7 \leq Pr \leq 16{,}700$ $Re_D \geq 10000$
Gnielinski (1976)	$Nu_D = \frac{\left(\frac{f}{8}\right)(Re - 1000)Pr}{1 + 12.7\left(\frac{f}{8}\right)^{\frac{1}{2}}(Pr^{\frac{2}{3}} - 1)}$ where $f = (0.79\ln(Re) - 1.64)^{-2}$	$0.5 \leq Pr \leq 2000$ $2300 \leq Re \leq 5 \times 10^6$
Chilton&Colburn (1934)	$Nu_D = 0.125 f Re Pr^{1/3}$ where $f = (0.79\ln(Re) - 1.64)^{-2}$	$0.7 \leq Pr \leq 160$ $Re_D \geq 10000$ $L/D \geq 10$
Ghajar&Tam (1994)	$Nu_D = 0.023 Re_D^{0.8} Pr^{0.385} (L/D)^{-0.0054} (\mu_b/\mu_w)^{0.14}$	$3 \leq L/D \leq 192$ $7000 \leq Re \leq 49000$ $4 \leq Pr \leq 34$ $1.1 \leq \mu_b/\mu_w \leq 1.7$

All correlations were almost within $\pm 10\%$. The closest values (almost $\pm 5\%$) were given by Ghajar and Tam (1994) correlation. Figure 3.9 shows the comparison for the correlations. As it can be seen, the experimental setup is working properly.

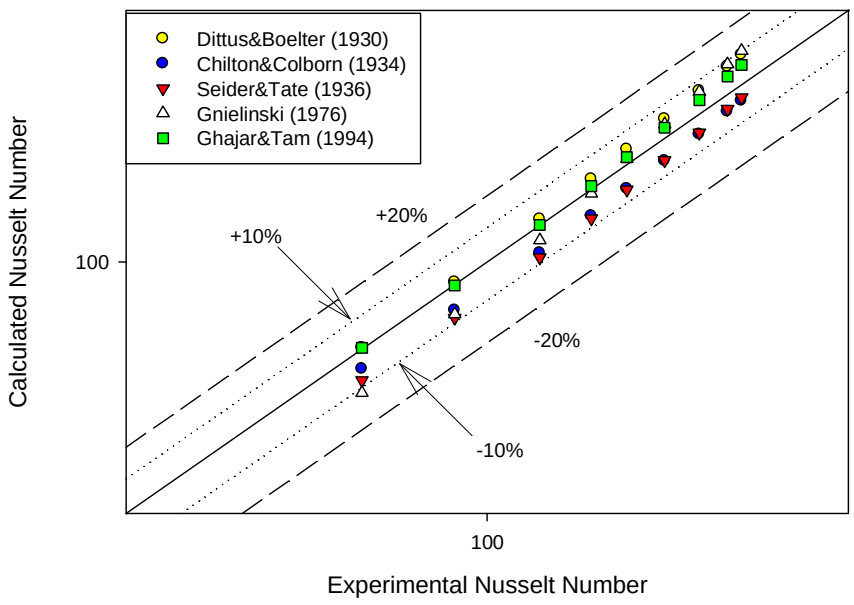

Figure 3.9 Single Phase Heat Transfer Measurements against the Correlations

CHAPTER IV

RESULTS AND DISCUSSION

4.1 Pressure Drop

It is already known that some properties like void fraction and flow pattern are strongly related to the pipe orientation. The present study has contributed to the understanding of two-phase frictional pressure drop in downward orientation. One of the main goals was to determine if there were significant behavior differences between horizontal and vertical two-phase frictional pressure drop and to see how successful two-phase pressure drop correlations were against the experimental results. Another important point was to observe the effect of flow patterns on the pressure drop. For this purpose, it is better to make the analysis for the flow pattern by flow pattern and represent the influence of different parameters on the flow.

Before representation and discussion of the results, a more detailed explanation of some related concepts and parameters, briefly introduced in previous chapters, is required for the sake of clarity and completeness. One of the most common and important concepts used in two-phase flow studies is void fraction. The void fraction is defined as the ratio of the volume occupied by the gas to the total volume.

$$\alpha = \frac{Volume_{Gas}}{Volume_{Total}} \tag{4.1}$$

Based on the observations of previous researchers, void fraction has been accepted as a very influential parameter related to both pressure drop and heat transfer of two-phase flow.

A similar concept for liquid phase is known as liquid hold up and defined as:

$$H_L = \frac{Volume_{Liquid}}{Volume_{Total}} = 1 - \alpha \tag{4.2}$$

The next one is the liquid pressure drop multiplier which is defined as:

$$\Phi_L^2 = \frac{(\frac{\Delta P}{\Delta L})_{Frictional\ two\ phase}}{(\frac{\Delta P}{\Delta L})_{Frictional\ liquid}} \tag{4.3}$$

Like void fraction, the liquid pressure drop multiplier is a well-known non dimensional number firstly defined by Martinelli et al. (1944). It is commonly used in two phase pressure drop analysis and correlations and shows the ratio of two phase pressure drop to single phase liquid pressure drop. The single phase liquid pressure drop is based on the assumption that, if liquid phase exists alone in the pipe. Then, it can be calculated from a suitable pressure drop correlation like Churchill (1977). The same idea can also be applied for a gas pressure drop multiplier which is less common. Different pressure drop multiplier approaches can also be seen in the literature.

As it is known, another way to represent the pressure drop is to use Darcy or Fanning friction factors. The usage of the friction factor concept is a tradition in the engineering community for single phase flow; however, there is no agreement on the

definition and the usage of the concept for two-phase flow. To use the concept, one must define two-phase density and the definition may differ from researcher to researcher. One of the simplest definitions for the two phase density is to use no slip two-phase density which is defined as follows:

$$\rho_{TP} = \frac{1}{\frac{x}{\rho_G}+\frac{(1-x)}{\rho_L}} \tag{4.4}$$

Now, a two-phase friction factor can be defined as follows:

$$f_{TP} = \frac{(\Delta P_{Two\ Phase\ Frictional}/\Delta L)D^5\pi^2\rho_{Tp}}{8(_L+_G)^2} \tag{4.5}$$

4.1.1 Analysis Based on Flow Patterns

There were mainly five flow patterns observed by Bhagwat (2011) who used the same experimental setup for the same orientation: bubbly, slug, falling film, froth, and annular. Basically, the flow pattern map of Bhagwat (2011) was followed in the present study to label the flow pattern of each run. A detailed definition of each flow pattern and flow ranges for each flow pattern was given in his work. The relation between flow patterns and pressure drop and the comparison of flow patterns in terms of pressure drop multiplier will be the main interest in this section.

Bubbly Flow: The bubbly flow can be characterized by the flow of almost homogenously scattered gas bubbles through a continuous liquid phase. In vertical downward flow, these bubbles are formed around the pipe axis and away from the pipe wall. The frictional pressure drop in this regime increases by increasing liquid or gas flow

rates and approaches single phase liquid frictional pressure drop by decreasing superficial gas Reynolds number (Figure 4.1).

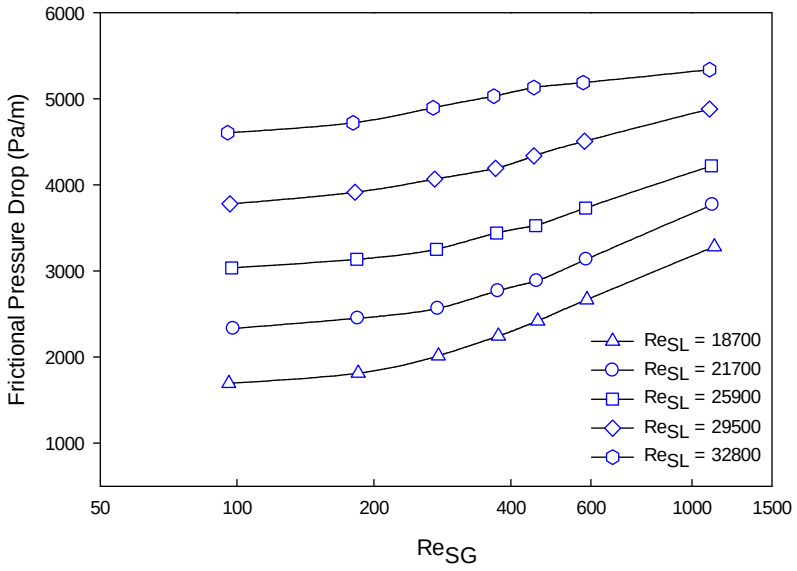

Figure 4.1 Variation of Frictional Pressure Drop against Re_{SG} in Bubbly Flow Regime

The link between pressure drop and liquid hold up for constant gas flow rates is given in Figure 4.2. Most researchers prefer to plot pressure drop against Re_{SG} or Re_{SL}. However, as it can be seen, liquid hold up or void fraction can provide a better perspective to represent the behavior of two phase flow in some cases since this parameter allows us to get smoother trends. This also proves the strong connection between void fraction and pressure drop. Please also notice that how the pressure drop almost keeps its magnitude in spite of reducing water mass flow rate when we approach to the bubbly-slug transition region.

The relation between liquid hold up and liquid pressure drop multiplier for constant gas flow rates is given in Figure 4.3. An exponential-like decay occurs for the

liquid pressure drop multiplier that approaches to one with the increase in liquid hold up. The pressure drop multiplier values of bubbly flow regime are relatively low when compared with other flow patterns. One can explain the reason due to the low gas flow rates or void fraction values in the bubbly flow regime. This is a correct argument in some degree but if we use suitable parameters like liquid hold up and liquid pressure drop multiplier for comparison of flow patterns, we will see that some flow patterns, in spite of sharing some common void fraction values or gas flow rate ranges, show different characteristics. This shows that the relatively low liquid pressure drop multiplier values are not only related to low gas flow rates or void fraction but also the geometrical structure of the flow. This will be discussed in the slug flow section.

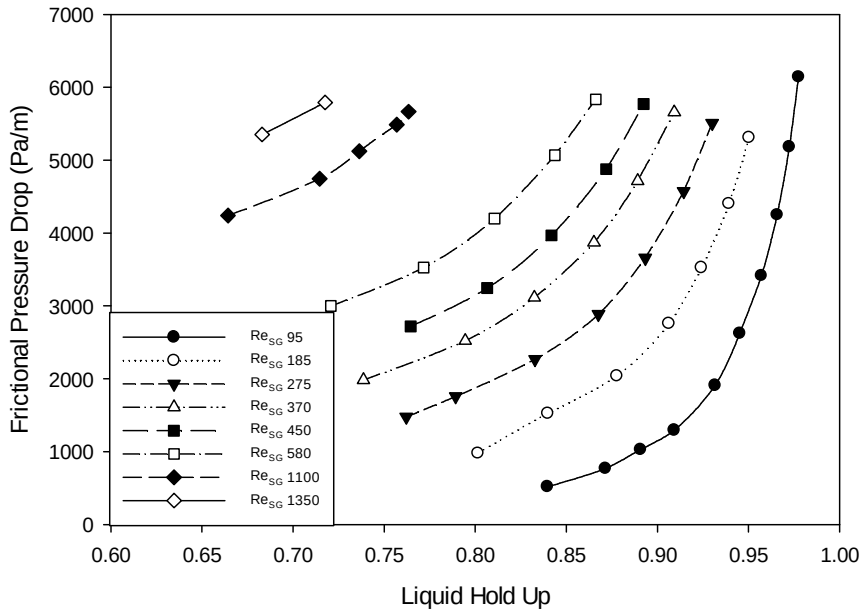

Figure 4.2 Variation of Frictional Pressure Drop against Liquid Hold-up in Bubbly Flow Regime

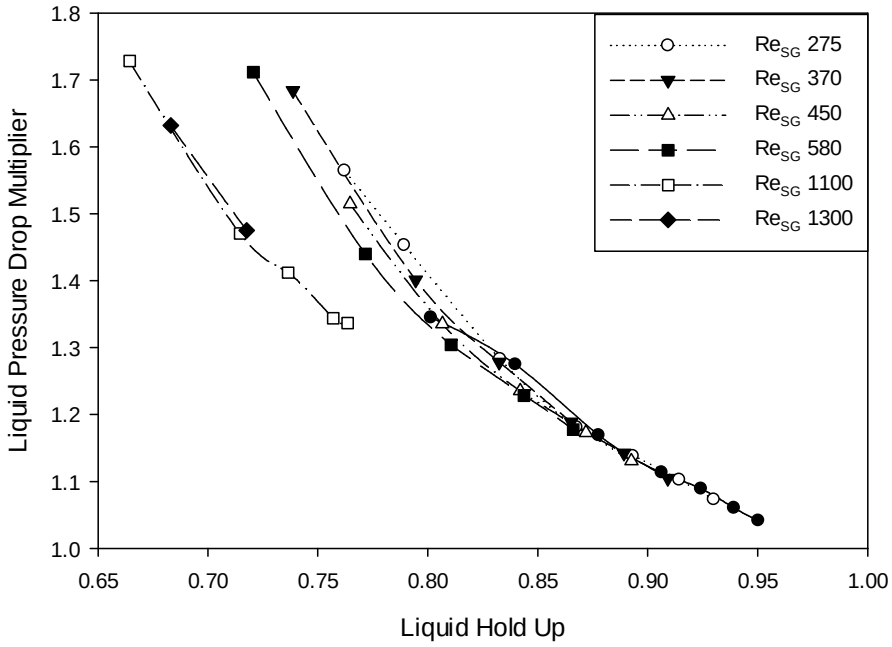

Figure 4.3 Variation of Frictional Pressure Drop Multiplier against Liquid Hold-up in Bubbly Flow Regime

Slug Flow: The slug flow, as it can be understood by its name, is characterized by slug shaped gas masses flowing through in the liquid phase in the pipe. This slug formation of gas phase causes high fluctuation in the pressure drop. Frictional pressure drop against Re_{SG} is given in Figure 4.4. As it can be seen in the figure, a very nonlinear behavior can be observed in this region. It starts to behave even more and more unstable especially for lower flow rates as shown on the left graph. On the other hand, the trend becomes more acceptable with increasing the liquid flow rate as shown on the right graph. This also generally makes difficult to predict pressure drop for this flow pattern. The reason may be due to the strong influences of different factors like gravity, buoyancy, and inertia forces. It is obvious that more research is needed to understand the behavior of this regime.

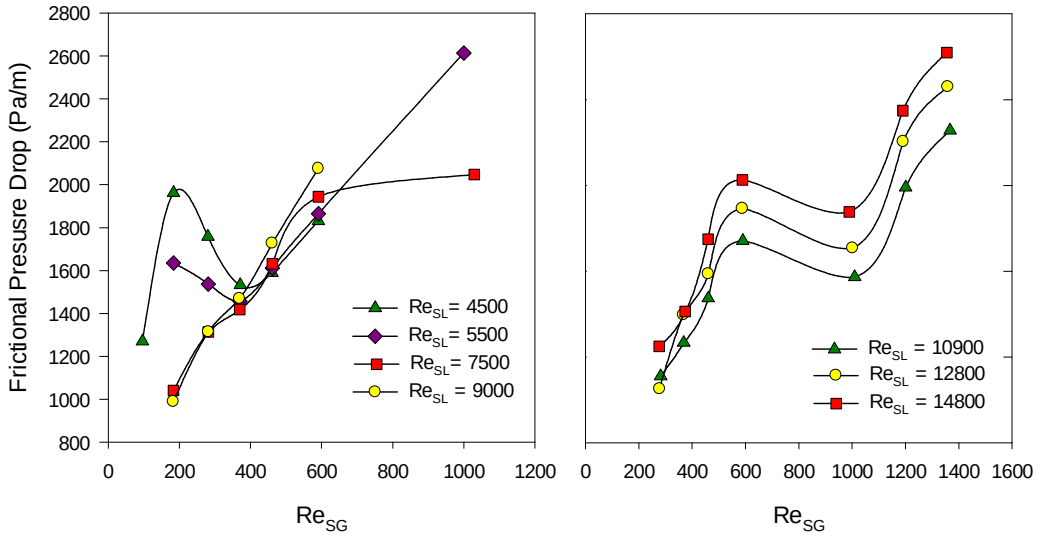

Figure 4.4 Variation of Frictional Pressure Drop against Re_{SG} in Slug Flow Regime

As we said earlier, superficial Reynolds number may not be sufficient to see the big picture. If we plot two-phase frictional pressure drop which was defined earlier against liquid hold up, a more understandable trend can be obtained (Figure 4.5).

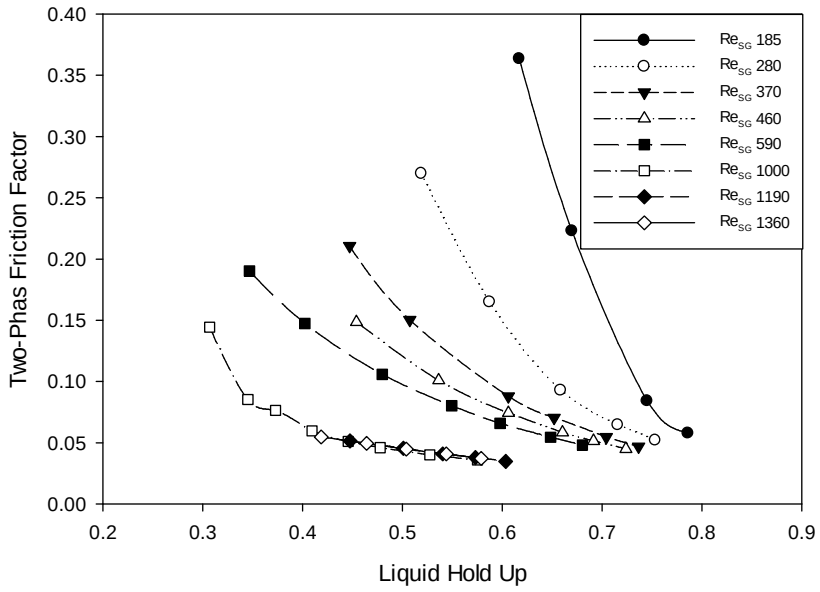

Figure 4.5 Variation of Two-Phase Friction Factor against Liquid Hold-up in Slug Flow Regime

The relation between liquid pressure drop multiplier and liquid hold up is given in Figure 4.6. If we return to Figure 4.3, we can clearly see the effect of the two different flow patterns on the flow. Now, we can compare bubbly flow against slug flow for the specific liquid hold up range (0.65-0.8) in terms of liquid pressure drop multiplier. This shows how the formation of gas masses effect liquid pressure drop multiplier for the same void fraction values. Since slug flow and bubbly flow occur in different flow rates, this concept allows a better way for the comparison. Consequently, one can expect not higher pressure drop values but much higher liquid pressure drop multiplier values for the slug flow when compared against the bubbly flow for the same liquid hold up range.

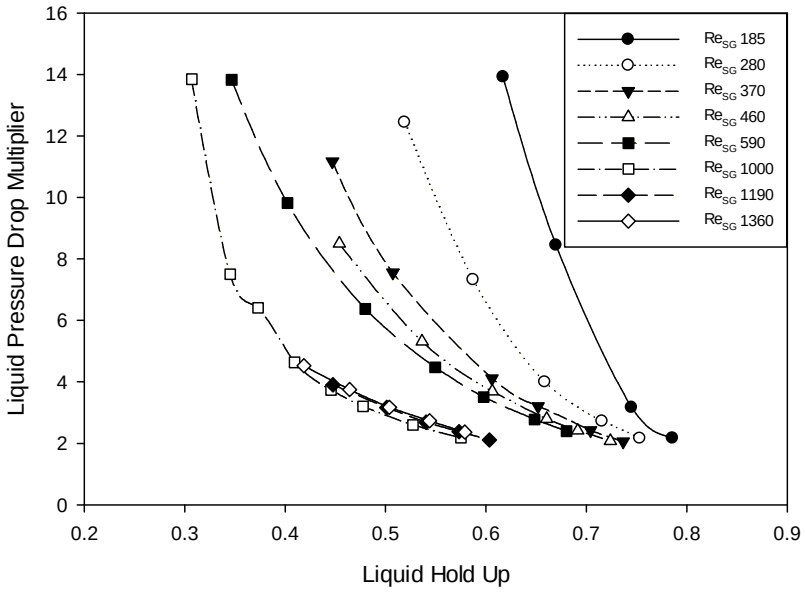

Figure 4.6 Variation of Liquid Pressure Drop Multiplier against Liquid Hold-up in Slug Flow Regime

Froth Flow: The froth flow allows more mixing and lead to higher interfacial interaction between liquid and gas phases. Therefore, higher frictional pressure drop occurs in this regime when compared to the regimes discussed previously. There is an almost linear

increase in pressure drop trend by increasing gas flow rate (Figure 4.7). Moreover, the frictional pressure drop has even more linear relationship with liquid hold up for this regime (Figure 4.8).

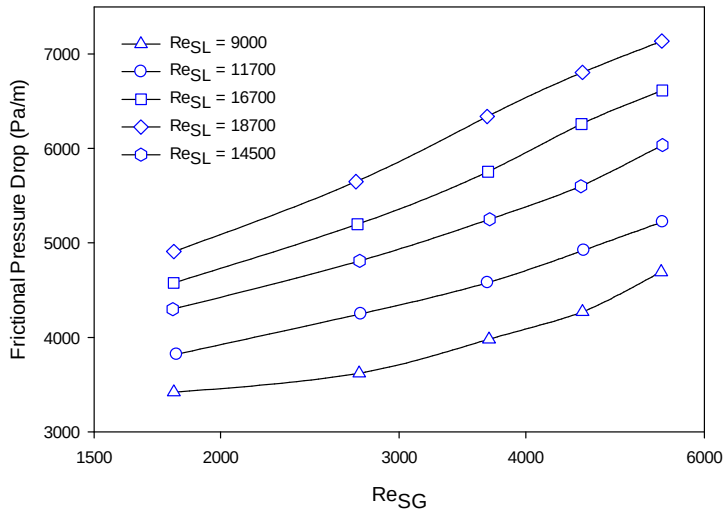

Figure 4.7 Variation of Frictional Pressure Drop against Re_{SG} in Froth Flow Regime

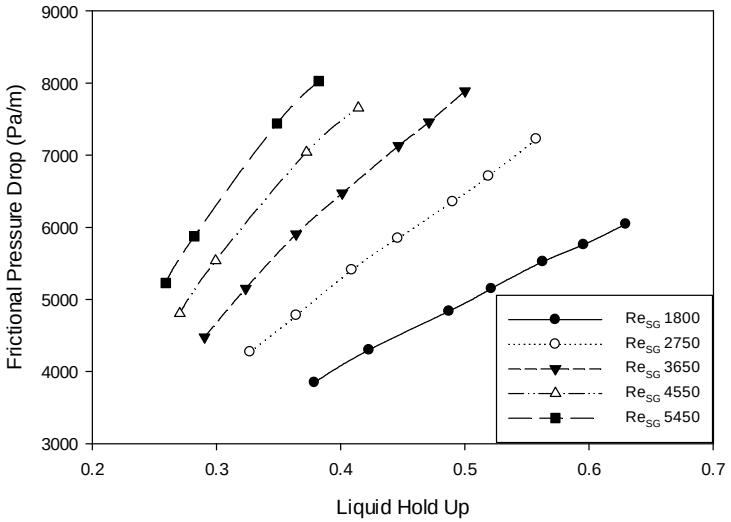

Figure 4.8 Variation of Frictional Pressure Drop against Liquid Hold-up in Froth Flow Regime

The froth flow occurs at relatively higher gas flow rates when compared against the bubbly and slug flows. So, once again liquid hold up may give better understanding in terms of comparison of liquid pressure drop multiplier values (Figure 4.9). It may not be fair to compare froth flow against bubbly flow in terms of liquid pressure drop multiplier since it does not give a clear idea about the effect of the flow patterns. However, we can make a similar conclusion as we made before for the bubbly flow against the slug flow. The liquid pressure drop multiplier values in the froth flow regime are smaller than the liquid pressure drop multiplier values of slug regime for the same liquid hold up range (0.3-0.6).

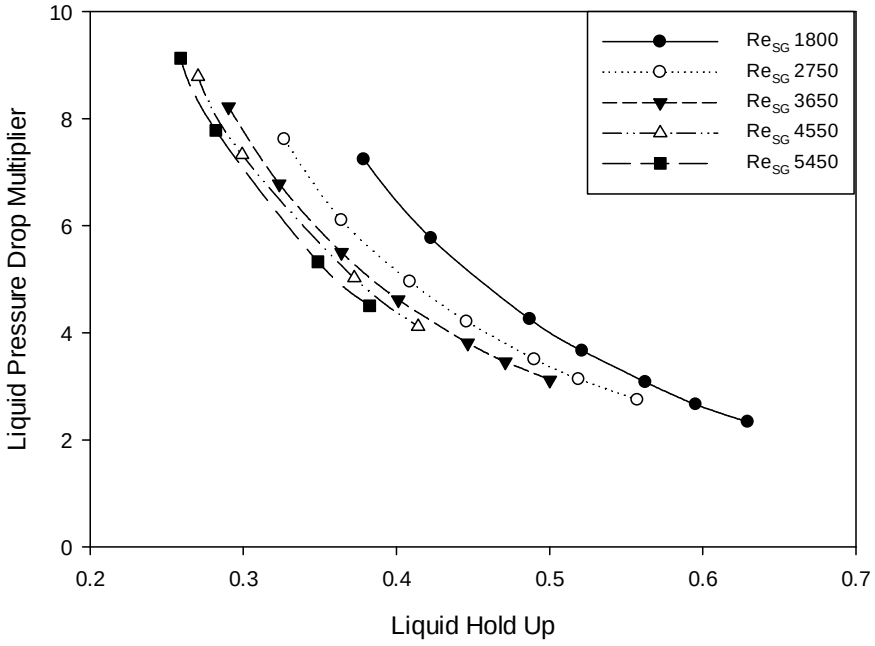

Figure 4.9 Variation of Liquid Pressure Drop Multiplier against Liquid Hold-up in Froth Flow Regime

The two-phase friction factor concept can allow us make further analysis. We observe an almost linear decrease by increasing liquid hold up in Figure 4.10. This may explain the

effect of buoyancy when we return to Figure 4.5 for comparison against slug flow. There was an exponential increase in terms of two phase friction factor by decreasing liquid hold up. Since mass flow rates are much higher in the froth flow regime, inertia force is more dominant. Unlike the slug flow, the froth flow may be effected less from buoyancy for the same liquid hold up range when we reduce liquid flow rate.

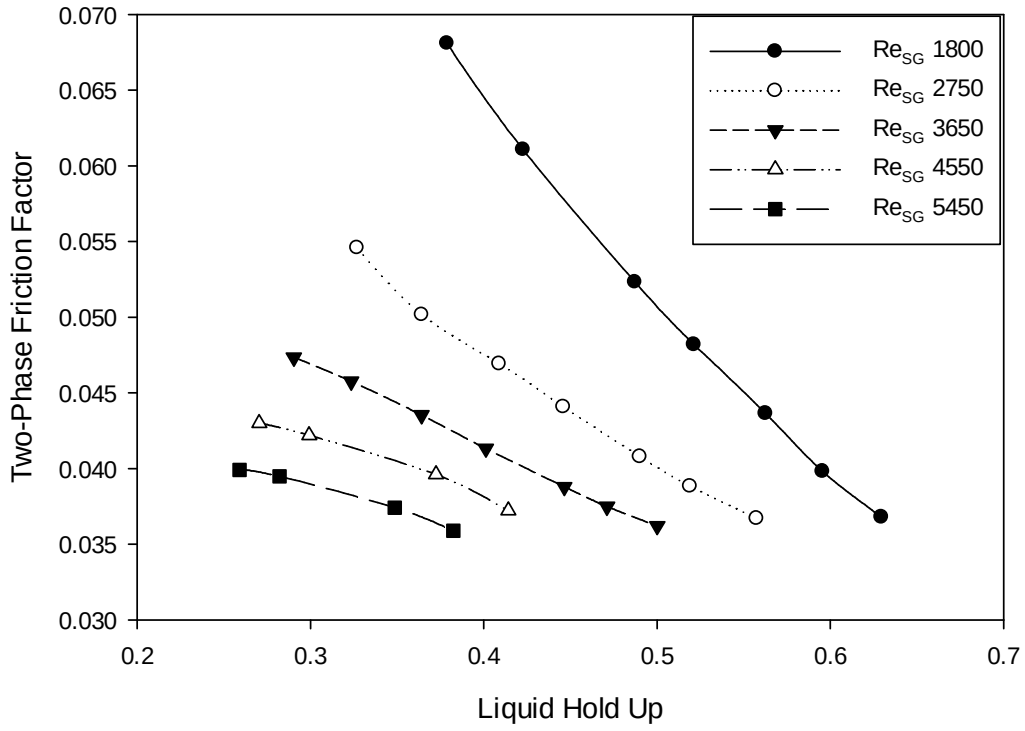

Figure 4.10 Variation of Two-Phase Friction Factor against Liquid Hold-up in Froth Flow Regime

Falling Film Flow and Annular Flow: The falling film flow is unique to downward flow orientation. In this regime, a thin liquid film streams over the pipe surface while the gas phase flows through the pipe core freely. The annular flow is similar to falling film flow. However, gas flow rates and generally void fractions are much higher. The liquid phase is pressed between gas core and pipe wall in annular flow. On the other hand, dry

spots can be observed in the falling film flow. As a result, the interfacial friction between phases for annular flow is higher compared to falling film. The frictional pressure drop and liquid pressure drop multiplier plotted against Re_{SG} is given in Figure 4.11. One of the interesting phenomena observed in the present study about the falling film flow is that the pressure drop does not change significantly by increasing gas flow rate until the falling film-annular transition region. Moreover, the liquid pressure drop multiplier for the falling film can be compatible to the liquid pressure drop multiplier of the annular flow.

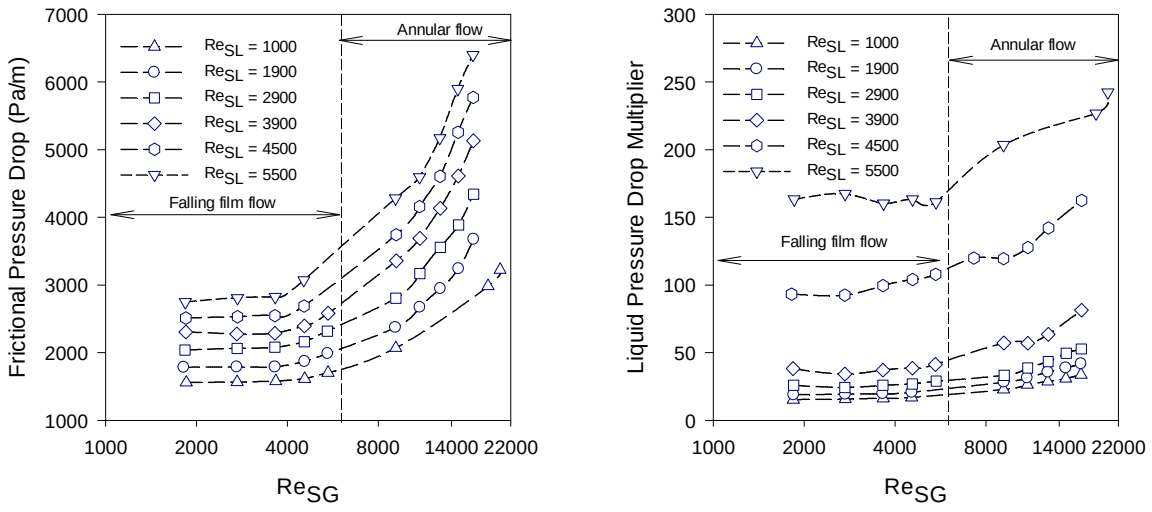

Figure 4.11 Variation of Frictional Pressure Drop against Re_{SG} in Falling Film and Annular Flow Regimes

The relation between liquid pressure drop multiplier and liquid hold up for the falling film and the annular flow regimes is given in Figure 4.12 and Figure 4.13, respectively. As we mentioned before, the liquid pressure drop multiplier values for the same liquid hold up range are compatible for these two regimes. It may be understandable if the geometrical structures of flows are considered. Both flows look similar according to

human perception. However, we need to talk about the reason behind the comparable liquid pressure drop multiplier values. For both of the flow regimes, liquid flow rates are generally lower compared to others. In falling film regime, gas flow rates are lower than annular gas flow rates. Interfacial friction between phases is also low for the falling film. As we see in the comparison of the froth flow to the slug flow, buoyant force is playing a critical role again here. For some flow rates of falling film regime, buoyant force is very compatible to inertia and the gas mass can even hold its position for several seconds in pipe. This behavior was observed by Bhagwat (2011). The drag force acting on the gas phase was not sufficient and there was an almost equilibrium between the drag force and buoyant force. When this happened, the water started to slip over the air while the air mass held its position and started to spin by not moving through the pipe in some area close to the pipe wall and the falling film layer broke down. In another word, the air was acting like a kind of blockade in the pipe. This behavior was causing a sudden rise in the system pressure. When the system pressure became overwhelming, the air was forced to move again and the flow returned to its normal condition. This phenomenon had occurred periodically for the flow. Because of the instability of the flow, the void fraction measurements were not able to be performed for some runs in the falling film region in Bhagwat (2011). This shows how buoyant force can be influential in this regime. When we increase the gas flow rates and enter to the annular flow regime, the effect of buoyancy starts to decrease. The gas phase becomes more dominant and does not need the liquid phase to move. It starts to compress the liquid phase towards the wall and even perform drag force on the liquid phase. So, the drag force changes its direction. However, the wall friction kicks in this time in annular flow. As a conclusion, the reason behind the

high liquid pressure drop multiplier values for the falling film is different and should be related to the changing role of the acting forces.

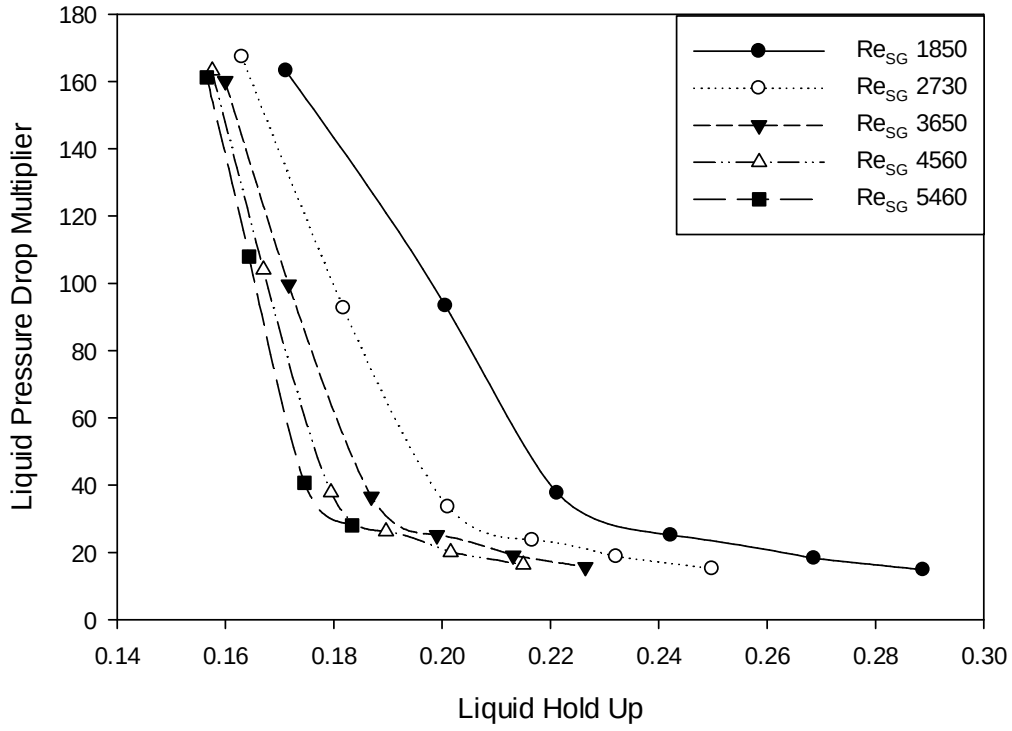

Figure 4.12 Variation of Liquid Pressure Drop Multiplier against Liquid Hold-up in Falling Film Flow Regime

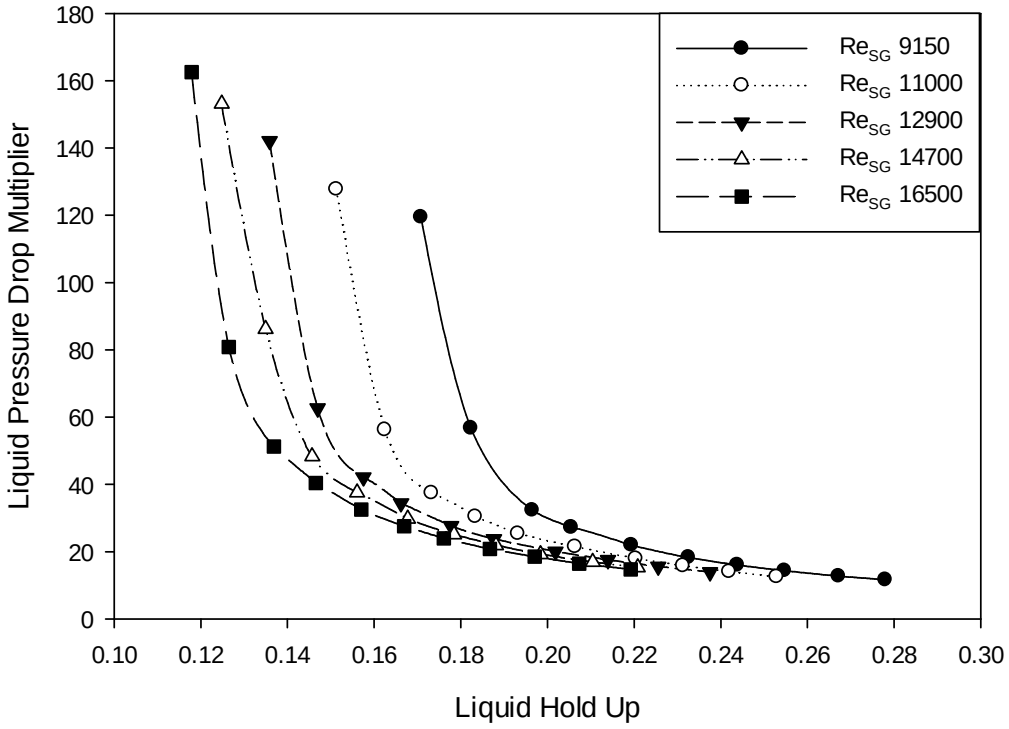

Figure 4.13 Variation of Liquid Pressure Drop Multiplier against Liquid Hold-up in Annular Flow Regime

4.1.2 Performance of Correlations for Pressure Drop Results

In this part, the performance of some of the well-known two phase pressure drop correlations was checked against the frictional pressure drop data and the weakness of the correlations was discussed.

Several correlations are available in the literature. The Lockhart&Martinelli (1949) correlation is one of the famous and commonly used correlations. The approach can be considered as the foundation of the separated model since most of the researchers followed the same path by trying to modify and improve the correlation. In spite of

handling phases separately, the solution approach is based on superficial single phase pressure drop. By introducing the second phase into the single phase, pressure drop is supposed to increase. So, there should to be a link between superficial and two phase pressure drop and it may be expressed as a function. Another attempt is homogenous model. The model is based on the idea that two phases may be treated like a homogenous phase. Therefore, two phase density and two phase viscosity also have to be defined. Using a well-known single phase pressure drop correlation is a tradition for this model. One of the most preferred is The Colebrook-White (1939) equation. Several researchers have tried to define different two phase densities and viscosities in order to fit their data and keep the constants of Colebrook-White (1939) equation in order to stay in Moody Chart region. Beside these models, using similarity analysis is another way as shown by Dukler et al. (1964).

A dozen correlations were tested against the data. Although some correlations were successful in some flow patterns, none of them was able to produce satisfactory results for all regions. Another unexpected finding is that some correlations like Beggs and Brill (1973) or Mukherjee (1979), which are commonly used in the oil industry for different inclination angles, were far away from predicting the data. Only three correlations produced some favorable results that could be noticed. The first one is Cicchitti et al. (1960) correlation. Despite its simple structure, the correlation was successful in the bubbly and annular flow regions (Figure 4.14). However, the results for slug flow and the falling film were not desirable. Again, most of the data for the froth flow regime were not in ±15% error band. Some other homogenous model correlations also produced closer results; however, it was observed that the modifications of the

homogenous model made by most researchers either did not improve the results or even made them worse. This shows that there might be a fundamental mistake or at least insufficiency related to the model since the modifications of the model do not help us in terms of making progress.

Lockhart and Martinelli (1949) produced comparable results with Cicchitti et al. (1960) (Figure 4.15). Although it was not successful in annular region as Cicchitti et al. (1960), the results for the froth flow regime were more reasonable. Once again, the falling film and the slug regions were seen as the most problematic regions.

Shannak (2008) showed best performance (Figure 4.16). Unfortunately, it was not able to produce good results for the falling film and the slug regions either.

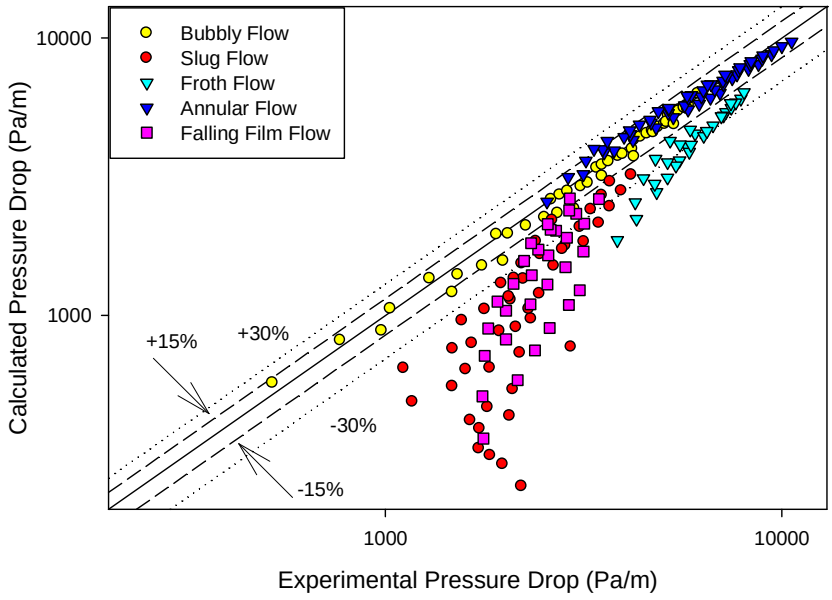

Figure 4.14 Comparison of Pressure Drop Data against Cicchitti et al. (1960) Correlation

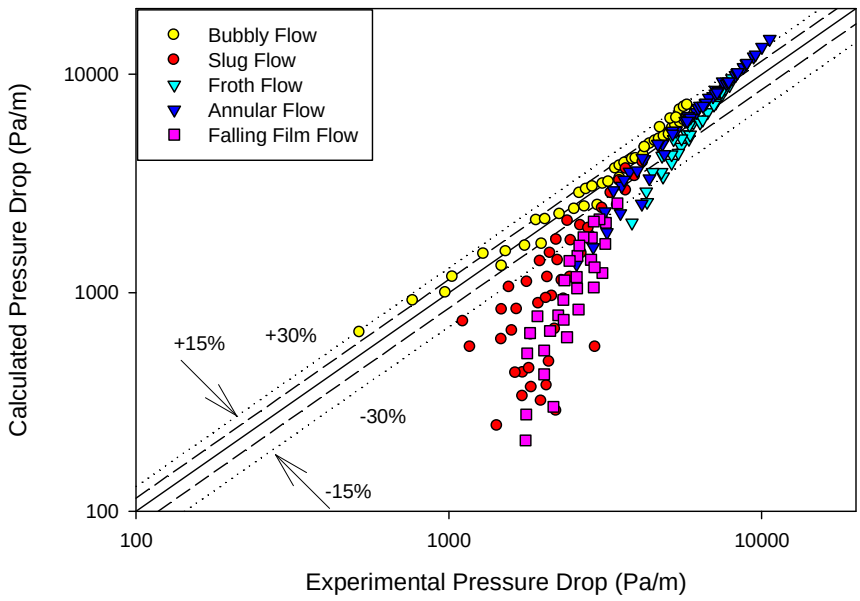

Figure 4.15 Comparison of Pressure Drop Data against Lockhart&Martinelli (1949) Correlation

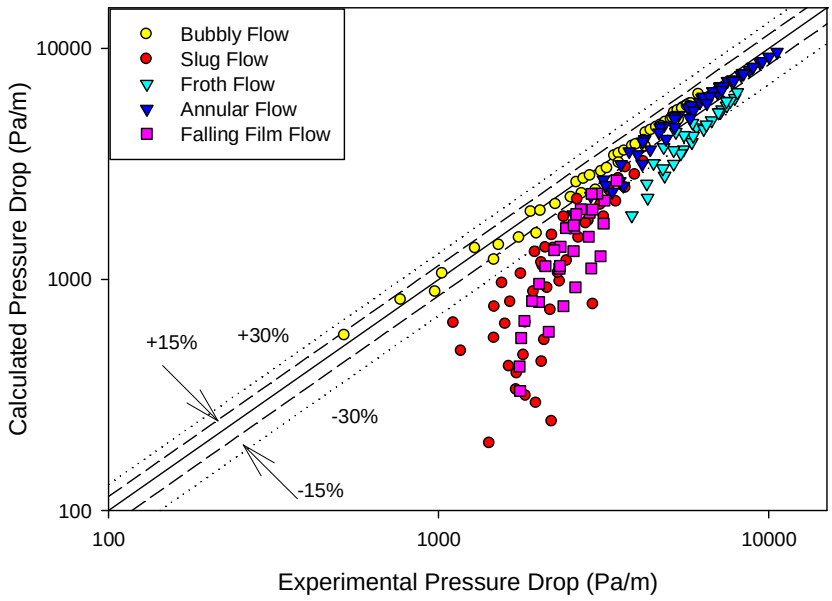

Figure 4.16 Comparison of Pressure Drop Data against Shannak (2008) Correlation

Now, it can be seen that there is a common failure in some regions for all correlations. Another observation is that downward two phase flow causes significantly higher pressure drop in some regions if we assume that these correlations are working reasonably for horizontal flow. The data of Oshinowo (1971) also validates this statement. A comparison against Shannak (2008) correlation is given in Figure 4.17. Moreover, as we mentioned in the literature review section, Oshinowo (1971) stated that Lockhart&Martinelli (1949) failed against his data and the correlation was able to produce some reasonable results only for bubbly and annular flow regimes similar to our findings.

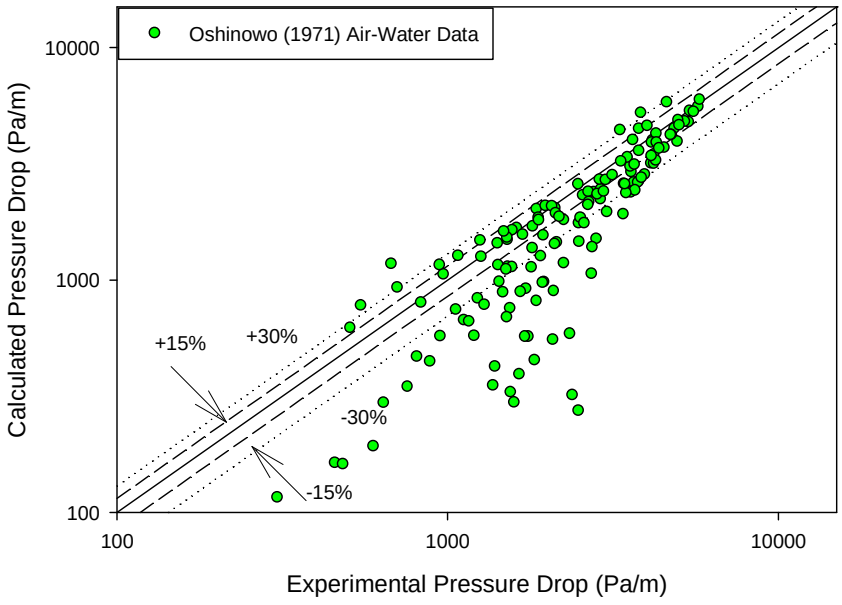

Figure 4.17 Comparison of Oshinowo (1971) Air-Water Pressure Drop Data against Shannak (2008) Correlation

As it can be noticed, the correlations generally fail for lower pressure drops. In another word, low flow rates cause unpredictable pressure drops for the correlations.

There are several reasons why the available two-phase pressure drop correlations fail. The first issue is that two-phase frictional pressure drop does not behave monotonically unlike single phase pressure drop. In another word, it is possible to increase frictional pressure drop by decreasing flow rate of one of the phases. We also observed this behavior especially in the transition regions. For instance, the frictional pressure drop increased by decreasing liquid phase for the constant gas flow rate in the bubbly slug transition region for lower gas flow rates. The sign of the slope of the trend can change. The transition in two-phase, should not be confused with the laminar-turbulent transition of single phase. Moreover, several transition regions exist for two-phase flow. Also, the flow pattern concept sometimes becomes insufficient to explain the transition.

Now, let us explain what the observation made above means in terms of correlations. As we mentioned earlier, the homogenous model is based on the definition of two phase thermo-fluid properties. Therefore, the friction factor concept provides a bridge between single phase and two-phase. However, the issue is that it is not always possible to stay in Moody Chart region. From an engineer's point of view, the parameters like two-phase density or viscosity are supposed to have a value between the values of the properties of liquid and gas phases. On the other hand, it can lead to very high friction factor values for some regions. Then, the homogenous model will fail. Otherwise, one should define an artificial two phase density or/and viscosity values that have to be even higher than liquid phase's. In another word, we assume an imaginary fluid which is more viscous and/or dense than the liquid phase. A similar situation exists for the separated model too. If we return to Figure 4.4, the reason why this model fails can also be understandable. As it can be seen, the trend is not monotonic. Some local minima may

exist for the trend. The separated flow model assumes that flow rates should be directly proportional to pressure drop. However, it is not true. A change in the flow rate for both liquid and gas phases can lead to an inverse effect on pressure drop. Moreover, the transition regions are not only dependent on flow rates. All the other thermo-fluid properties jump into the fray.

Consequently, there are critical transition zones for two-phase flow and we have not been able to produce a general solution for the problem yet. It is obvious that we should approach the case from a different angle.

4.2 Heat Transfer

The heat transfer measurements were not done simultaneously with the pressure drop measurements in this study since both measurements have specific restrictions and specific requirements that should be followed in order to get reliable data. However, almost the same mass flow rates were examined for both cases. This gave us a good understanding about the relation between heat transfer and pressure drop and showed that downward non-boiling two phase heat transfer could be a very good candidate for use of Reynolds analogy to predict two-phase flow heat transfer coefficient. Even, it could be considered that the pressure drop data validated the heat transfer data in an indirect way. As was done in the previous section, we will present our analysis flow pattern by flow pattern and try to show the relation within the pressure drop data. Some well-known two phase heat transfer correlations will also be examined against the data.

4.2.1 Analysis Based on Flow Patterns

Five flow patterns will be analyzed in this section once again. The heat transfer data had less data points (165) compared to the pressure drop data (207) since both heat balance error and some safety issues existed for the heat transfer measurements. Still, the data is sufficient to identify the similarities between the pressure drop and heat transfer characteristics of downward two phase flow.

Bubbly Flow: Two phase heat transfer coefficient against superficial gas Reynolds number is given in Figure 4.18. The two phase heat transfer coefficient is increased by injecting more gas into the system in this region. Single phase heat transfer coefficient lines are also drawn in the figure for comparison by using Sieder and Tate (1936) correlation. As it can been seen, an interesting phenomenon takes place here. The heat transfer rate can be reduced by gas injection for some flow rate ranges in the bubbly region for downward flow. Please remember that the bubbly flow is generally characterized by its homogenous structure. So, maybe we can make a connection with natural convection to understand this behavior. In natural convection, only one phase exists however the driving force is the density difference. Although the reason for the density difference and the mechanism for natural convection are different, it may still help to understand the reduction in two phase heat transfer rate for some points in bubbly region. There are some studies that show the effect of natural convection in vertical tubes. Interestingly, natural convection can reduce heat transfer rate for a heated pipe in downward flows since it is considered as opposing flow.

One can argue that this is not so significant in terms of $\frac{h_{TP}}{h_L}$. However, we observe a similar situation in terms of liquid pressure drop multiplier for some points in the pressure drop data. In spite of having high void fraction (α>0.2), a few bubbly points' pressure drop multiplier values were almost one. Moreover, the fluid combination and/or diameter can also make this reduction more significant as Oshinowo (1971) data showed that it was possible to see significant reductions. This phenomenon can be remarkable for some industrial applications. For instance, reduced heat transfer rate can be beneficial for oil industry since the oil is wanted to preserve its temperature against decomposition in oil pipe lines.

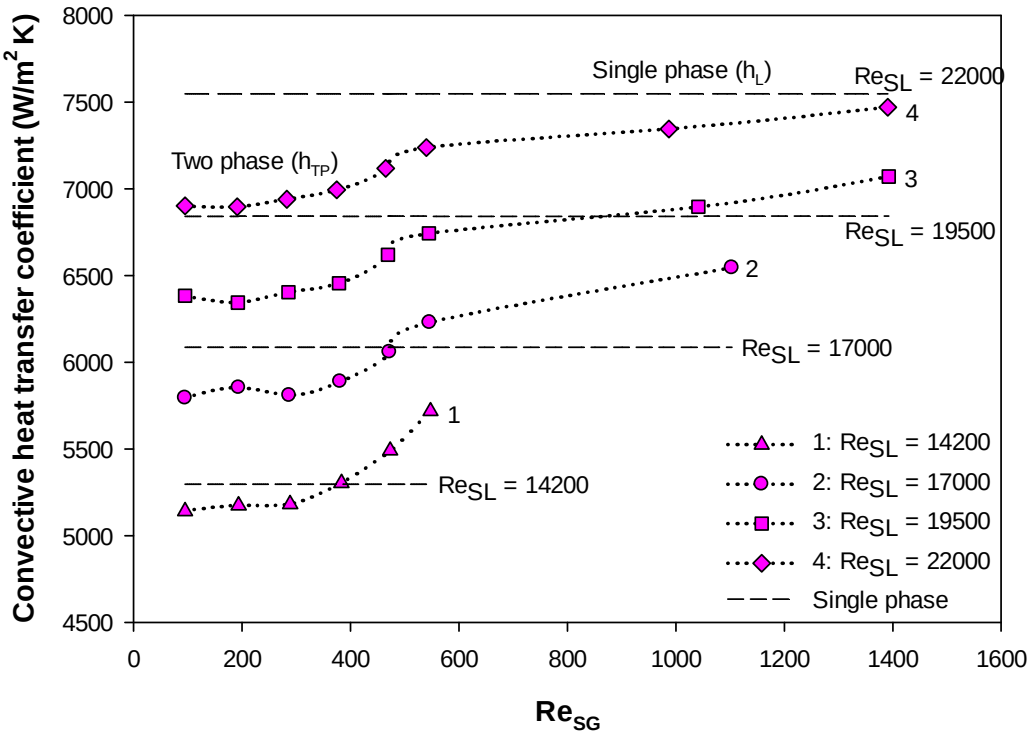

Figure 4.18 Variation of Two-Phase Convective Heat Transfer Coefficient against Re_{SG} in Bubbly Flow Regime

Slug Flow: The trend of heat transfer coefficient versus superficial gas Reynolds number is given in Figure 4.19. In the figure, we see an increase for the heat transfer coefficient by gas injection. The second important point is that a transition occurs at $Re_{SG} \approx 600$ since the slope of the lines change significantly. We do not observe any reduced heat transfer rates similar to some points in bubbly flow regime when compared to single phase heat transfer rates in this region.

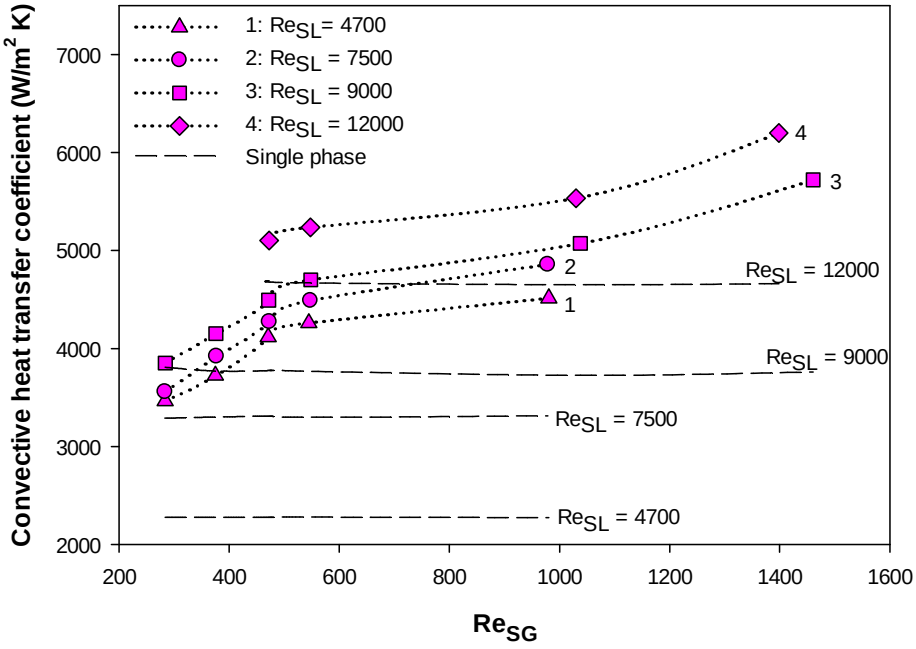

Figure 4.19 Variation of Two-Phase Convective Heat Transfer Coefficient against Re_{SG} in Slug Flow Regime

At this point, it is better to show slug to bubbly transition region since the neighborhood of these two regimes are critical to understand the heat transfer characteristics of low flow rates (Figure 4.20). In Figure 4.20, the slug points are colored with red and the bubbly points are colored with yellow. Similar to the pressure drop,

there is a sharp change in the heat transfer behavior. It is very interesting to observe that the heat transfer can be enhanced by reducing liquid phase flow rate for very low flow rates. Please notice how the lines become normalized when we increase gas flow rate. We know that if we are talking about convective heat transfer, the movement of fluid is the characteristic of this type of heat transfer. The question arises here that how the heat transfer can be enhanced by reducing the flow rate of the liquid phase which its thermo physical properties are superior than the gas phase in terms of the importance to the heat transfer mechanism. The answer may be the velocity profile of the flow. We reduce the velocity and the average thermo physical properties of the flow by reducing the liquid phase flow rate; however, the velocity profile of the flow is changed drastically by entering into a non homogeneous structure from a homogenous (bubbly) structure which its velocity profile is quite similar to single phase flow.

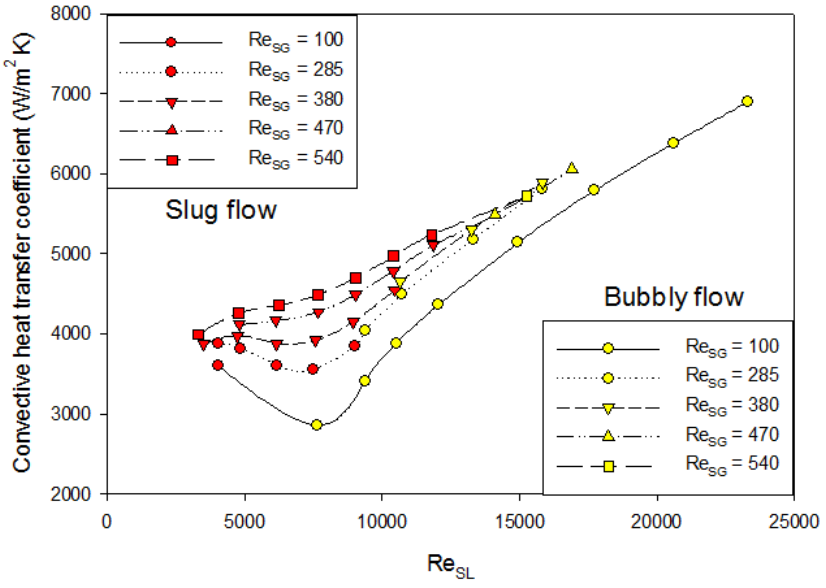

Figure 4.20 Variation of Two-Phase Convective Heat Transfer Coefficient against Re_{SL} in Slug to Bubbly Flow Transition Regime

Froth Flow: The froth flow behaves smoothly as expected. If we recall the pressure drop results for this regime (Figure 4.7), the heat transfer behavior is not a surprise. The heat transfer coefficient in this regime is increased slightly by adding more gas into the system as shown in Figure 4.21. Unlike slug flow, it seems that this regime is not sensitive to the gas flow rate since it can only be formed for higher liquid and gas flow rates. Consequently, small increments in gas flow rates do not make a big difference in froth flow regime.

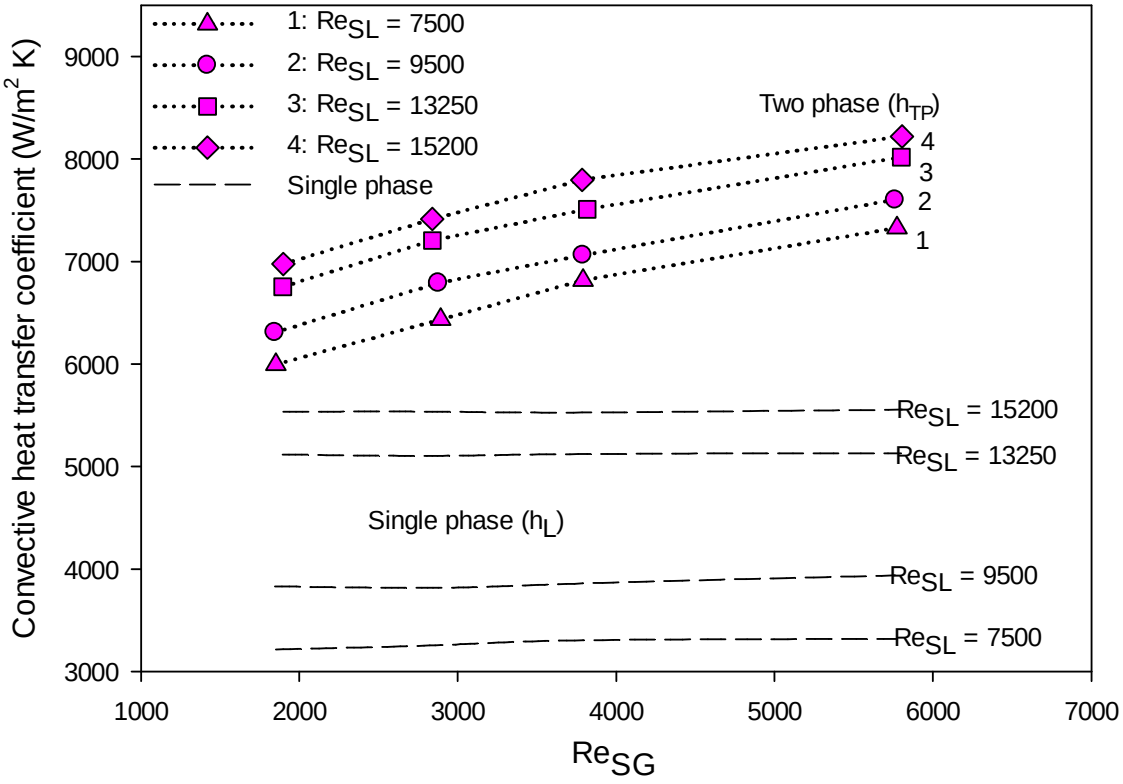

Figure 4.21 Variation of Two-Phase Convective Heat Transfer Coefficient against Re_{SG} in Froth Flow Regime

Falling Film Flow: The two phase heat transfer coefficient against superficial gas Reynolds number for falling film regime is given in Figure 4.22. Maybe, the falling film flow can be considered as the most problematic regime in terms of heat transfer for downward flow. This region is very sensitive to especially liquid flow rate. As it was mentioned earlier, dry spots can occur in this regime and the heat transfer rate is affected significantly in case of the loss of liquid-wall contact. There are two ways to bypass these critical points due to dry spots. The first one is that the heat transfer can be enhanced by increasing liquid content. More gas injection into the system is the second way. So, we introduce the gas into the system and it can cause dry spots in the beginning. Further gas injection may reduce dry spots by pushing the liquid phase towards the wall. As a result, one can expect to see such ups and downs in the heat transfer trend for falling film regime similar to one shown in Figure 4.22.

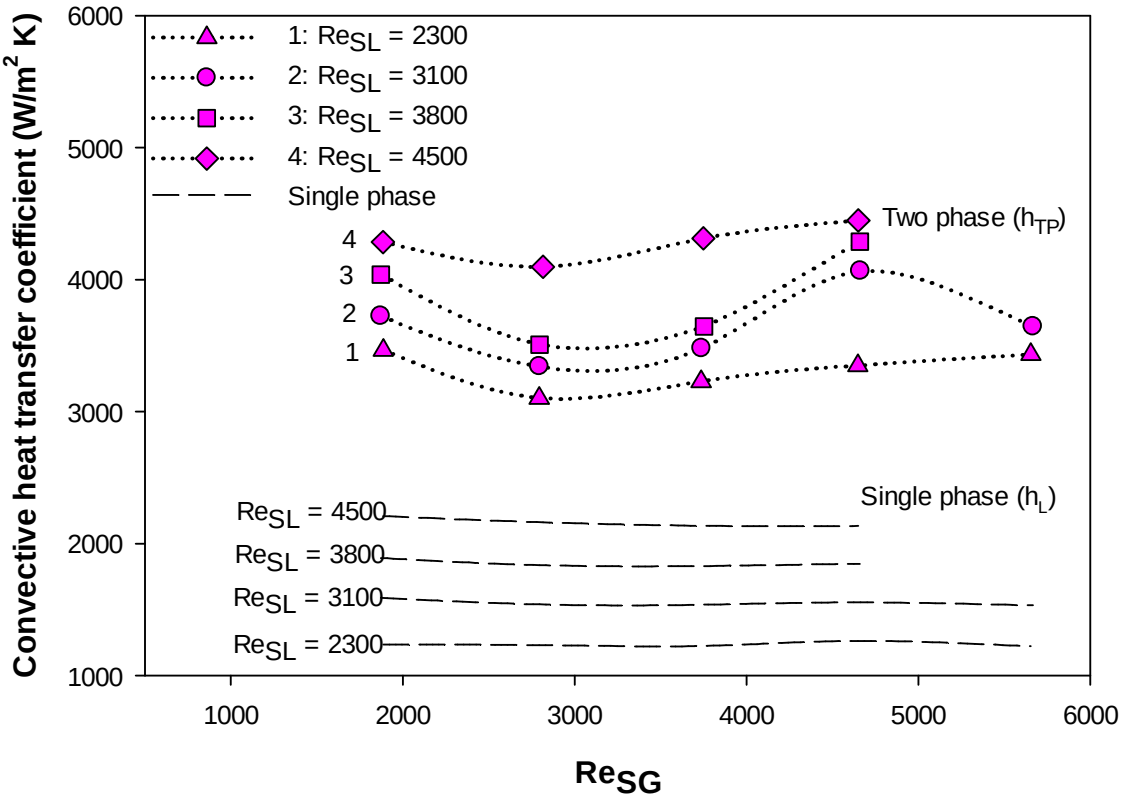

Figure 4.22 Variation of Two-Phase Convective Heat Transfer Coefficient against Re_{SG} in Falling Film Flow Regime

Annular Flow: The two phase heat transfer coefficient increases monotonically in annular flow regime (Figure 4.23). One of the reasons of this monotonic increase is that the annular flow is the extreme region for two phase flow. Further gas injection will lead to annular-mist and eventually mist flow will occur. Unlike other regimes, introducing more gas in annular flow regime will cause small increments in void fraction. This is the reason why a small linear slope in the figure is observed in spite of introducing large amounts of gas into the system. Abnormalities in the trend may be seen when we

approach annular-mist transition region since the liquid film layer starts to break up.

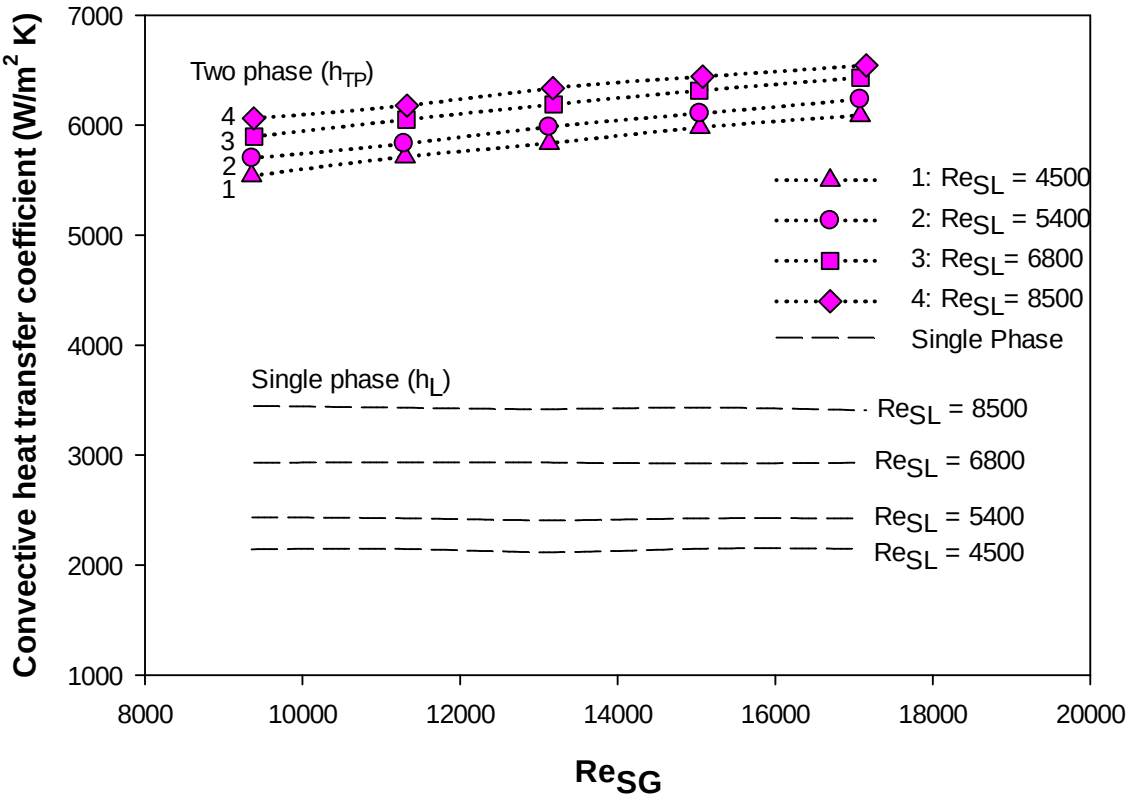

Figure 4.23 Variation of Two-Phase Convective Heat Transfer Coefficient against Re_{SG} in Annular Flow Regime

4.2.2 Performance of Correlations for Heat Transfer Results

The performance of correlations against the heat transfer data was seen more reasonable when compared to the performance of pressure drop correlations against the pressure drop data. An overall performance of some well-known two phase heat transfer correlations is given in Table 4.1.

Table 4.1 Performance Analysis of Various Heat Transfer Correlations against the Data from Various Flow Patterns

Flow pattern	Bubbly (47 data points)				Slug (38 data points)				Froth (25 data points)				Falling Film (19 data points)				Annular (36 data points)			
Correlations	1*	2	3	4	1*	2	3	4	1*	2	3	4	1*	2	3	4	1*	2	3	4
Present Study	85	100	14.5	4.5	92	94.7	2.1	24.9	100	100	0.7	9.1	89.5	89.5	8.6	21.1	94.4	100	8.7	7.1
Aggour (1978)	0	0	39.9	6.1	18.4	36.8	29.4	16.8	0	0	51.7	9.5	0	0	68.8	20.4	0	2.8	69.9	19.5
Chu and Jones (1980)	0	23.4	40.3	15.4	50	71.1	20	16.4	96	100	4.7	6.8	21.1	36.8	39.8	23.9	2.8	22.2	35.5	6.1
Dorresteijn (1970)	0	0	47.4	7.7	26.3	47.4	28.1	19.2	0	0	56.6	13	0	0	57.7	18.3	2.8	5.6	66.1	21.5
Drucker et al. (1984)	0	59.6	32.2	12.1	13.2	31.6	36	11.8	92.2	100	2.2	11	63.2	89.5	16.5	32.6	8.3	38.9	33.6	9.4
Katasuhara and Kazama (1958)	0	0	85.3	33.1	0	0	96.4	20.2	0	0	48.5	7.6	0	0	138	56.6	0	0	60.9	7.1
Khoze et al. (1976)	0	0	216.7	36.9	0	0	185.2	47	0	0	238.7	37.1	0	0	227.9	41.1	0	0	255.1	38.5
Knott et al. (1959)	93.6	100	13.7	3.9	68.4	89.5	12.1	14.6	100	100	1.5	8.8	89.5	94.7	8	13.2	61.1	100	17.1	7.3
Kudiraka et al. (1965)	8.5	19.1	59.7	36.9	0	0	113.2	19.5	0	0	69.3	6.7	0	0	215.4	74	0	0	118.7	10.3
Kim et al. (2000)	78.7	100	16.1	3.9	92.1	97.4	4.7	12.6	60	96	18.4	7.2	47.4	68.4	27.1	16	38.9	69.4	21.9	13.9
Oshinowo et al. (1984)	0	0	136	20	0	0	119.1	26.7	0	0	107.4	18.6	0	0	119.7	31.2	0	0	94.9	16.2
Ravipudi and Godbold (1978)	55.3	74.5	19.7	15.7	97.4	97.4	4.3	8.9	72	100	17.1	5.5	0	0	80.5	29.8	0	0	70.2	5
Rezkallah and Sims (1987)	27.7	72.3	24.9	6.4	28.9	71.1	23.2	15.3	0	0	47.1	10.3	0	0	81.9	23	0	0	79.7	19.5
Shah (1981)	100	100	9.5	4	57.9	71.1	19.1	14.7	68	100	12.9	9.8	63.2	100	15.8	9.7	86.1	100	11.2	7.7
Tang and Ghajar (2011)	0	8.5	35.9	4.9	52.6	78.9	6.8	22.4	64	84	9.3	18.6	5.3	5.3	38.5	6.7	77.8	94.4	10.3	11.4
# Tang and Ghajar (2007)	95.7	100	10.2	5.4	55.3	68.8	148.8	13.9	44	72	21.6	11.5	5.3	21.1	34	7.9	63.9	92.7	11.7	18.4
Ueda and Kanaoka (1967)	0	0	671	238.8	0	0	776.8	134	0	0	49.5	3.4	0	0	126.8	40.6	0	0	102.9	10
# Vijay et al. (1982)	100	100	2.7	5.1	36.8	57.9	27.3	14.1	20	48	31.4	11.8	0	5.3	48.7	7.6	0	0	52.2	7

Correlations based on Reynolds analogy, *Note: In the above table, numbers 1,2,3 and 4 refer to: 1=% number of data points within ± 20 % error bands, 2=% number of data points within ± 30 % error bands, 3=Mean absolute error (%), 4= Standard deviation

As expected, most of the correlations were able to predict the bubbly flow region reasonably well. Shah (1981) and Tang&Ghajar (2011) correlations were the best for this regime. The slug flow regime was once again one of the difficult regimes to predict for the correlations. Still, the results can be considered satisfactory for the majority of the points. Kim et al. (2000) and Ravupudi&Godbold (1978) were the most satisfactory correlations for the slug flow. Chu&Jones (1980) and Knott et al. (1959) can be recommended for the froth flow. Except for few points, Shah (1981) and Knott et al. (1959) were successful in the falling film regime. One of the main causes for those erratic points in the falling film regime could be the dry spot problem. For annular flow, Shah (1981) and Tang&Ghajar (2007) are recommended.

Knott et al. (1959) and Shah (1981) showed the best performance for the majority of the flow patterns. The performances of these two correlations are given in Figure 4.24 and Figure 4.25, respectively. In spite of more reasonable results unlike pressure drop correlations, the heat transfer correlations struggle to predict the heat transfer rates of lower flow rates. Most researchers tried to deal with these kinds of behavior changes for low flow rates by putting restrictions in terms of superficial Reynolds numbers that are only valid for single phase flow (Re = 2000). This does not look like an appropriate solution since if there are some transition regions for two phase flow as we have already shown, new dimensionless numbers should be identified to put more suitable restrictions for correlations. Interestingly, Shah (1981) assumed a lower Reynolds number (170) for his correlation. This shows that some researchers were aware of this problem and tried to minimize the error for their data by identifying different Reynolds number for the transition region. Unlike single phase flow, the existence of two phases makes it more

difficult to clarify the transition region since a lot of parameters may have influence on the transition region. Another interesting attempt was made by Chu and Jones (1980). They introduced $\frac{P_{atm}}{P_{sys}}$ into their correlation. Probably, they noticed an unexpected heat transfer rate for some lower flow rates for their data. Since low flow rates cause relatively lower system pressure, they might try to handle this problem in an indirect way. Further works are needed to enlighten this issue.

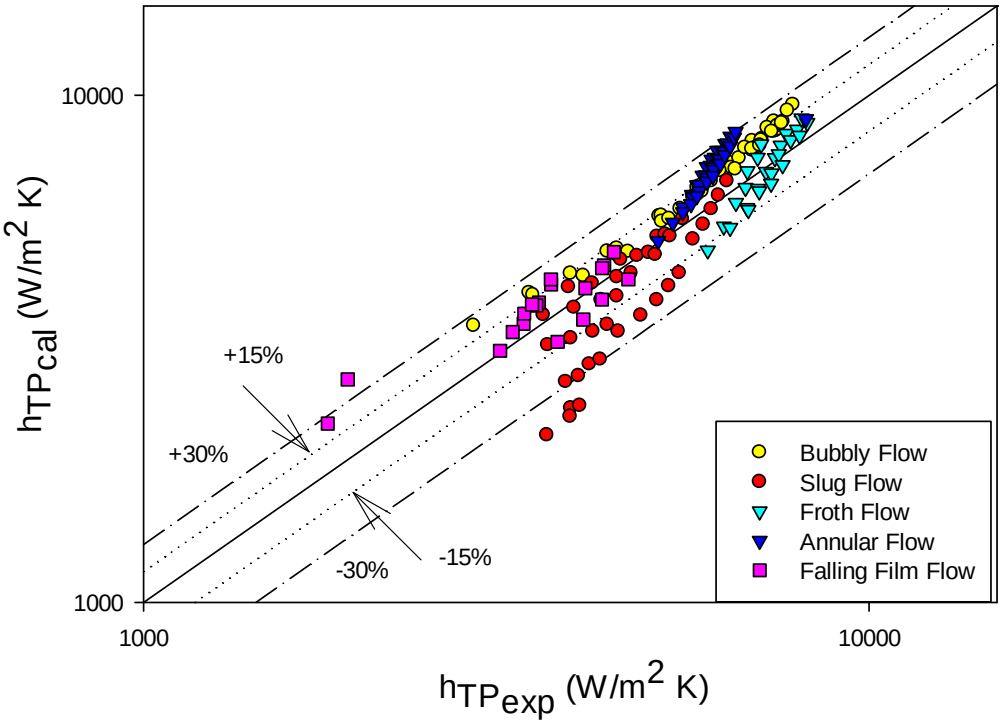

Figure 4.24 Comparison of Heat Transfer Data against Knott et al. (1959) Correlation

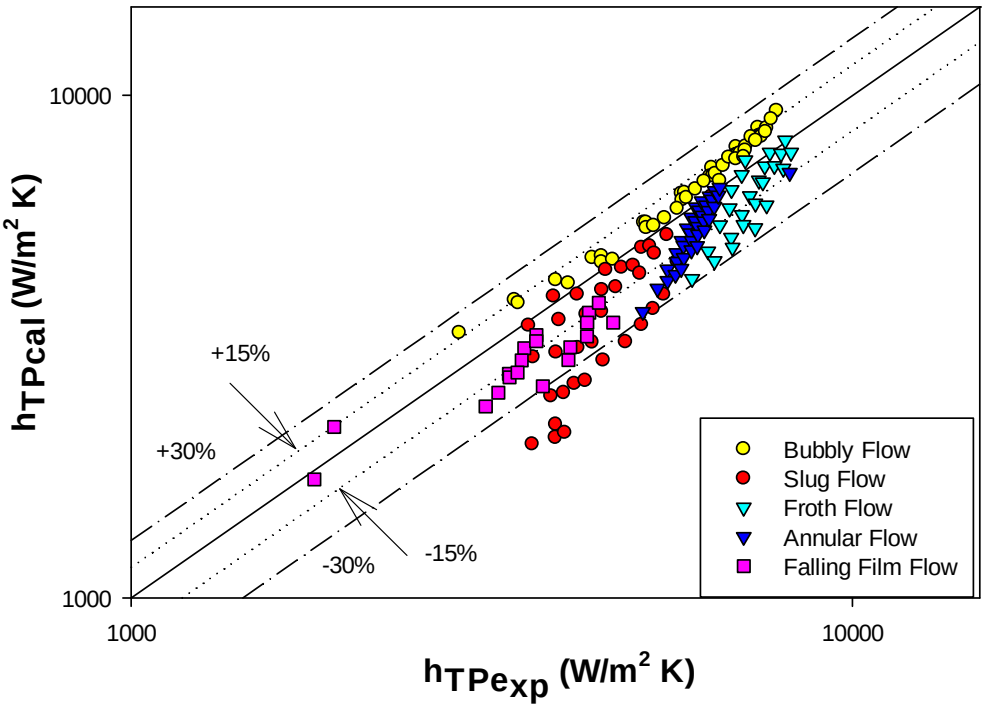

Figure 4.25 Comparison of Heat Transfer Data against Shah (1981) Correlation

Until this point, we have tried to show that Reynolds analogy might be the best way to deal with the problem if the pressure drop values were already known or were able to be calculated by a good pressure drop correlation. Since the approach is very effective for single phase, it can also be beneficial to calculate two-phase heat transfer. In a brief summary, Reynolds analogy depends on the relation between momentum and energy equation. Since both fluid phenomena are carried by advection, we expect to see analogical behavior. There were several studies for the usage of Reynolds analogy to calculate two-phase heat transfer. Yet, the studies were generally for horizontal or upward orientation. For this purpose, a simple but quite effective correlation is developed for downward flow. Since we can relate Nusselt number to Reynolds and Prandtl

numbers for single phase flow, a similar relation between two-phase pressure drop and heat transfer coefficient multipliers can be readily developed. Therefore, the proposed correlation is a simple power function of liquid pressure drop multiplier:

$$\frac{h_{TP}}{h_L} = \Phi_L^{0.55} \tag{4.6}$$

The performance of this new correlation is given in Figure 4.26. The correlation predicted most of the points which were not predicted by any of the correlations given in Table 4.1. Only two points from falling film regime were out of the desired range. This can be understandable due to the issue we have mentioned before.

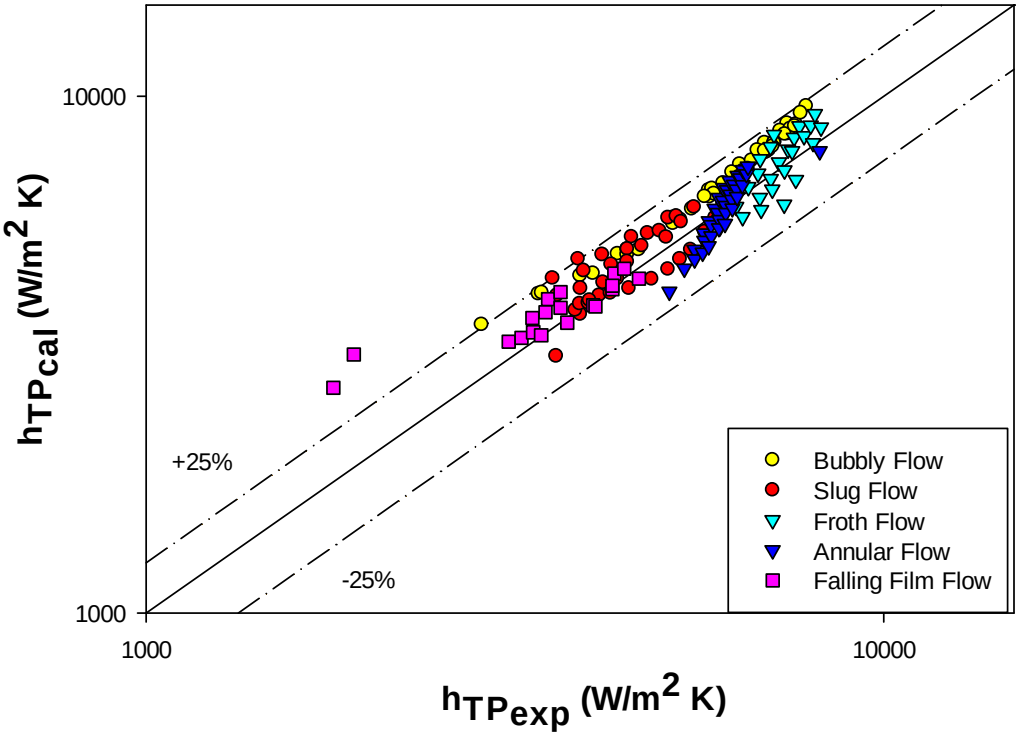

Figure 4.26 Comparison of Heat Transfer Data against Proposed Correlation Equation (4.6)

4.2.3 Comparison of Heat Transfer Characteristics of Downward and Upward Orientations

The present study is focused on downward flow; still, some heat transfer measurements were also conducted for upward two phase flow in order to get a better understanding of the influence of the direction of the gravity. Two-phase Nusselt number against superficial gas Reynolds number is given in Figure 4.27 for both upward and downward flows. Besides the same mass flow rates, the temperature difference between runs were kept to a minimum as much as possible. Our findings in this study are in agreement with other researchers. Upward heat transfer rates are generally higher than downward heat transfer rates. There are some regions in which the heat transfer rates of downward flow can be higher. The order of higher heat transfer rate with flow rate is as follows: upward-downward-upward. As it can be seen in the figure, the difference between the orientations is more significant for lower flow rates. The same observation was made by Oshinowo et al. (1984). It seems that the buoyancy effect is diminished by increasing liquid flow rates. Another interesting finding is the significant heat transfer difference for bubbly flow regime. This may validate our previous analysis related to the opposing flow concept for homogenous structure.

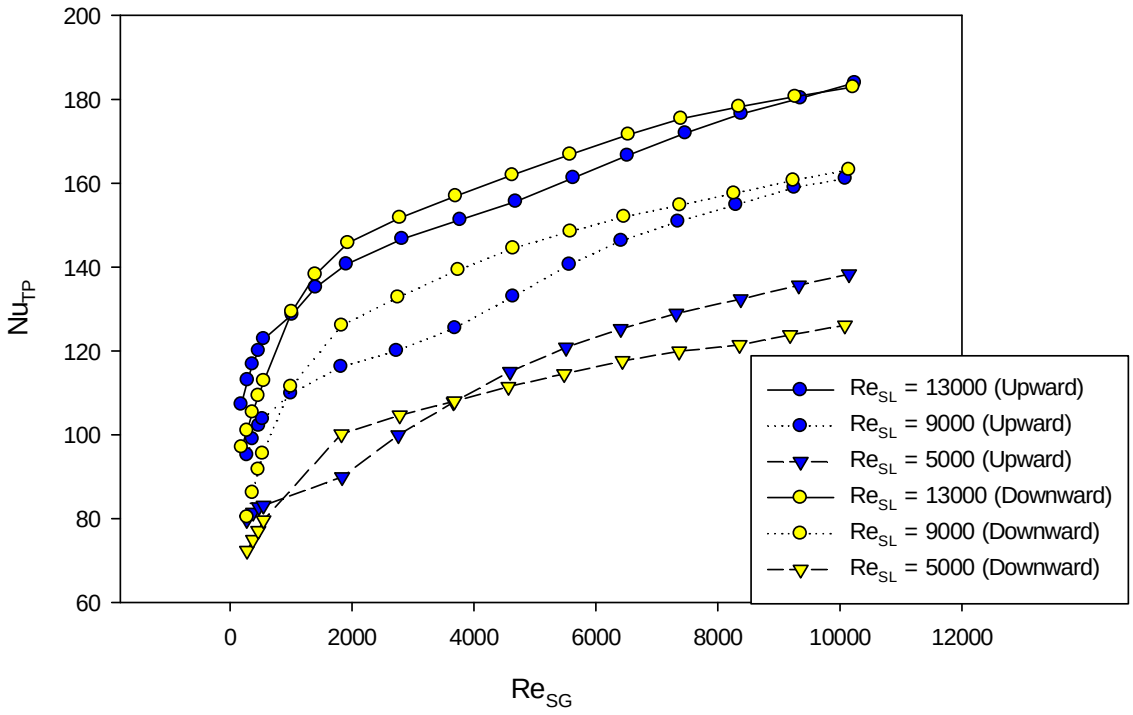

Figure 4.27 Comparison of Heat Transfer Rates Upward and Downward Two-Phase Flows

4.3 Recommendations for Modeling

In Chapter 4, different correlations were tested against our experimental data and the efficiency of the correlations was generally flow pattern dependent especially for pressure drop data. This problem is not only related to our experimental data but a general case that almost every experimental data have some uniqueness. This is the reason why a correlation can only produce reasonable results only for the experimental data that is used to develop that correlation. So, these correlations generally provide solutions for specific cases.

If a more robust model is wanted, we should approach the case in a different way. We already know that Reynolds analogy can be used effectively. So, developing a good model for pressure drop will solve the problem. At least, the idea behind that model can be modified to develop a model for heat transfer.

Let us begin our analysis by asking the most important question. What is missing? Engineering community developed two concepts in order to solve the problem. One of them is void fraction and the other one is flow pattern. Void fraction is the volume ratio of phases. It is a mathematical concept that we can express in terms of numbers. First researchers developed simple correlations by using this concept in order to produce a solution. However, although a relation has been seen, this did not enlighten pressure drop and heat transfer phenomena sufficiently. Then, we have started to visualize flow and developed flow pattern term. We looked at the flow and gave names to the flow depending on the geometry and grouped our data based on flow patterns. We became closer to the solution because we started to see similar behaviors for each flow pattern. At least, this concept was more useful. Then a lot of researchers started to develop correlations based on flow patterns. Unfortunately, flow pattern is not a concept that can be expressed in a mathematical way. It is very subjective. Secondly, both void fraction and flow pattern are actually outputs of the flow unlike flow rates, temperature, thermo-fluid properties. From application view point, it is not always possible to know flow pattern and there are no robust models to predict the pattern of flow. Once diameter and/or fluid pair are changed, we suddenly find ourselves in a new world. Consequently, flow pattern is also an output like pressure drop.

Now, let us think the relation between pressure drop and flow pattern. Due to the position of phases in the pipe, we see a shape. What is the meaning of this shape for the flow? Simply, it is distribution of parameters like density, viscosity along the axis and the length of the pipe. Is this distribution random? No, it depends on some parameters like diameter, flow rates, surface tension and other thermo-fluid properties. But we do not exactly know how these parameters effect this distribution. Moreover, due to number of these parameters, it does not look easy to use all of these parameters to develop a model that defines this distribution. But maybe we can find an easier relation. We know that this distribution decides the characteristic of pressure drop but also vice versa. This is "chicken or egg" story. Suppose we have two not mixing liquids in a cup. We start to stir up and observe how these two fluids mix into each other. If we increase the speed, the mixture can become even more homogenous. For two phase flow, what is the mechanistic effect that forces these fluids mix into each other or decides homogeneity of the mixing? Can we use experimental pressure drop to understand flow pattern? One can ask what the purpose is. If we are able to find a relation between pressure drop and flow pattern in a mathematical way, we can get rid of flow pattern and obtain another concept that will do the job of flow pattern and this concept will be expressed as numbers. By using our experimental data, we can create a mathematical relation between pressure drop and this new concept. Since both pressure drop and this new concept will be related to each other, we can define two functions to observe their behavior against input variables and also their relationship. By that way, we can create two charts. After construction of these charts, we no longer need flow pattern. Next step, we check if we can observe a sensible pattern in these charts that allow a solution by an iterative approach. If that

works, we can transform these charts to equations by curve fitting. Finally, we can combine these two equations in order to get an implicit function that can be solved iteratively.

So, our aim is to develop a characteristic dimensionless number to use instead of flow pattern and/or void fraction. Now, let us consider an annular two phase flow. By using flow visualization or even experimental void fraction can be sufficient, we can draw a distribution line with respect to radius (Figure 4.28.).

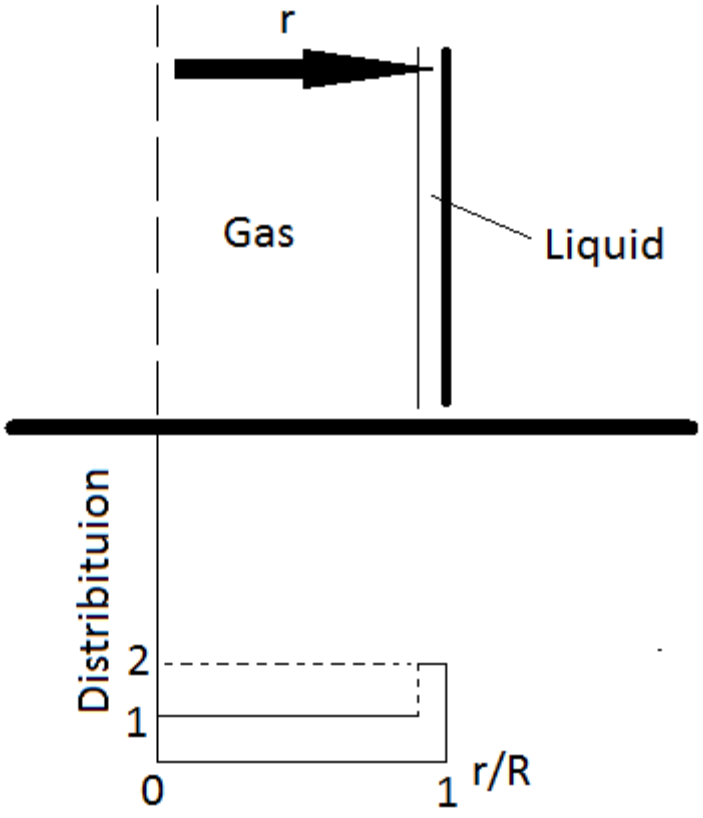

Figure 4.28 Distribution Line for Annular Flow

We can label fluids with numbers. For instance, the value of gas and liquid can be expressed as 1 and 2, respectively. Now, we have a distribution function (φ) that can be expressed as dimensionless diameter r^+ (r/R). For annular flow, due to the separation of phases, the line is supposed to be discontinuous that there will be a jump at the inter phase. Other flow patterns can also be expressed approximately in terms of distribution line. For instance for bubble flows, if it is not totally dispersed, there will be a liquid film near the wall, and a liquid-gas bubble core (that can be treated as homogenous) in the center. If void fraction and the thickness of the liquid layer are known, then we can draw an approximate distribution line similar to the annular flow. Other flows that show a periodic behavior like slug can even be approximated by averaging by help of using void fraction and flow visualization. After we obtain approximated distribution lines, we can go to the next step. Now, we need to find a way to express these distribution functions as a characteristic number (Shape Number). Let us assume that an unknown function (τ) exist that when we multiply this function with the distribution function and integrate with respect to diameter, we will obtain our desired shape number. If there is a discontinuity in the function, we can make partial integration.

$$\int_0^1 \varphi\, \tau\ dr^+ = Shape\ number \tag{4.7}$$

Please notice that we are not trying to make a numerical model. We are going to use numerical integration (if it is needed) just once to obtain a shape number and put the flow pattern out of the equation. Once, the model is built, there will be no need for any numerical integration.

Now, we can start to look for a relation to express this unknown function. This is the difficult part of the model. As we advocated earlier, using a function that consist of experimental pressure drop can be helpful. Let us give an example to explain. Most researchers use single phase liquid pressure drop to construct a bridge between two phase and single phase. Instead, let us use homogenous model and try to define a relation. Suppose we use homogenous model and calculate a two phase pressure drop. In this case, the distribution function is accepted as volumetric average and the value of φ is same at every point in r/R. On the other hand we get a different distribution and pressure drop from our experiment. Then, a relation may be found.

$$\varphi_{Homogenous} \leftrightarrow \Delta P_{Homogenous} \; and \quad \varphi_{Experimental} \leftrightarrow \Delta P_{Experimental}$$

Now, different dimensionless number or ratios can be tried. For instance:

$$\varphi_{model} = \varphi_{Experimental} - \varphi_{Homogenous} \tag{4.8}$$

And,

$$\tau = (\Delta P_{Experimental} - \Delta P_{Homogenous}) \times R^2 r^{+2} / \sigma \tag{4.9}$$

Now, we can multiply τ and φ_{model} and integrate with respect to r^+ (r/R). Please notice that, instead of surface tension (σ), other parameters can also be tried to make τ dimensionless. In this form, it is the ratio of shear stress difference to surface tension between phases. One can ask how about the question related to the magnitude of these two functions since we just gave arbitrary values (1, 2) to fluid phases. We are going to use dimensionless numbers that consist of thermo-fluid parameter of these phases. So, we expect to see different relations depending on the values which we gave to the fluids

before obtaining a shape number. We can return and reconsider these arbitrary values and can make some modifications for different fluid pairs if it is needed.

After we obtain shape numbers for all runs now we can create two charts and check how these shape numbers behave with two phase pressure drop. For instance, for the first chart, we can plot Shape number versus a dimensionless number which contains two phase experimental pressure drop in it and volumetric ratio. The second chart, we can plot $\Delta P_{Experimental}$ / $\Delta P_{Homogenous}$ against Shape number, density ratio, viscosity ratio or other possible dimensionless numbers. Then, we can check if a graphical solution is possible since we have two charts now and no longer need experimental pressure drop. $\Delta P_{Experimental}$ becomes $\Delta P_{Two\text{-}Phase}$ (unknown). We can assume homogenous flow and calculate homogenous pressure drop. We go to the first chart and find Shape number by using our initial guess (homogenous pressure drop) in the dimensionless number and volumetric ratio. After we find shape number, we go to the second chart and use shape number with other dimensionless number to find $\Delta P_{Two\text{-}Phase}$ / $\Delta P_{Homogenous}$ ratio. Now check if the solution is close enough to initial guess (which was homogenous pressure drop). After making some iterations, if we can find the experimental pressure drop, then the relation is obtained and we are ready for the next step. We can make curve fitting and obtain two equations. As in our example, it would be;

Shape number = f(Volumetric ratio, A dimensionless number that consists of two phase pressure drop,…)

$\Delta P_{Two\text{-}Phase}$ / $\Delta P_{Homogenous}$ = f(Shape number, μ_G/μ_L , ρ_G/ρ_L,…)

Finally, we combine the two equations by adding shape number into the second equation and we will have an implicit function that can be solved iteratively. By that way, solution becomes independent of flow pattern. Later, we can check the model against different experimental data that is obtained by using different fluid combinations and diameter sizes in order to see what kind of modifications can be made. Next step we can check the effect of roughness, effect of inclination (if it is possible to improve the model for all inclinations).

There is an important issue related to vertical flows that should be discussed. Since the total pressure drop is different than frictional pressure drop, one can argue the effect of the hydrostatic pressure drop on the distribution function and instead of using frictional pressure drop, it may be more favorable to use total pressure drop. If it is needed, frictional pressure drop can be calculated after finding total pressure drop. Based on the approach you are trying, it is possible to get negative pressure drop (which is already a case for downward pressure drop). Moreover, we may even observe negative frictional pressure drop for upward flow. The model can be flexible for those cases. For instance, shape number can also be calculated as negative in some cases depending on your model and it can make sense because we are dealing with sign changes for vertical flows. Beside this, we already saw that two phase pressure drop could be lower than superficial single phase pressure drop. In such cases, observing a sign change for shape number can be considered good.

There is one disadvantage of this approach that requires more effort and flow visualization is needed. However, if one can be sure about the flow pattern and if it is annular flow, then there is no need for flow visualization. Experimental void fraction

value will be sufficient. It would be more advantageous to check the model in annular flow before going for other flow patterns. If a relation is obtained and the model looks promising, we can go further. Otherwise it is possible to waste time. Also, if the aim of the study is modeling, measurements should be done based on the parameters that you are going to use for τ. For instance, we can regulate flow rates based on experimental pressure drop and try to obtain similar values. When we construct the first chart to see the behavior of shape number, it would be very advantageous to get smooth lines.

The shape number approach can also be useful for presentation of the data. Until now, there is no way to show all points clearly in a single graph. We have to use sub categories like flow patterns to show the trends. This causes discontinuity and makes the case difficult to see the big picture and understand transition regions. Actually, by using flow patterns, we just assume an imaginary axis. For instance, we check pressure drop against flow ratio or Reynolds number for only bubble flow. If the shape number idea works, we can make a better categorization based on a value.

CHAPTER V

CONCLUSIONS AND RECOMMENDATIONS

Two phase isothermal pressure drop and non-boiling heat transfer for vertical downward orientation were investigated experimentally in the present work. The measurements were conducted in a 0.01252 m diameter stainless steel tube and air-water fluid combination was used as working fluids. It was observed that both pressure drop and heat transfer depended on flow patterns, in other word, they depended on flow rates of gas and liquid. It was seen that especially low flow rates had different hydrodynamic and heat transfer characteristics. Some well-known correlations were also tested against the data. The most problematic regions were slug and falling film flows. Unlike pressure drop correlations, heat transfer correlations were able to produce more reasonable results. Still, more work is needed to develop flow pattern independent correlations for vertical downward orientation. The conclusions and the recommendations of the study are summarized in this chapter.

5.1 Conclusions of the Pressure Drop Measurement and Analysis

- Due to the homogenous structure, bubbly flow is a straightforward flow pattern. A monotonic increase was observed in frictional pressure drop by introducing more gas. Most of the correlations were able to predict this region easily. An interesting phenomenon took place in this regime. It was noticed that pressure drop could be reduced by injecting gas into the system for some flow rates. This was also supported by the data of Oshinowo (1971).
- Unexpected pressure drop results were seen in slug flow despite low gas injection. Especially for low flow rates, the error with respect to the correlations increased significantly due to the highly non linear behavior. It seemed that there was a transition dependence on both liquid and gas flow rates. The frictional pressure drop can even increase by reducing water or air flow rates in this bubbly to slug transition region.
- The data behaved monotonic and the frictional pressure drop increased almost linearly (especially against liquid hold up) by injecting more air into the system in the froth flow regime and no complications were observed in this regime unlike slug flow regime. However, the correlations were not successful once again for the low flow rates in this flow pattern. The error for these low flow rates against the correlations was relatively small when compared to the error for the slug flow regime; still, it was far away to be considered as reasonable.
- High frictional pressure drop and liquid pressure drop multiplier were observed for the annular flow as expected. The sensitivity against gas injection was relatively low for this regime since high amount of gas injection into the system

was required to observe a significant frictional pressure drop rise. Interestingly, despite using a homogenous model, some correlations (Shannak (2008), Cicchiti (1960)) were very successful to predict the frictional pressure drop.

- Due to its uniqueness, the falling film flow may be considered the most interesting regime that was observed in this study since it can only be seen in vertical downward orientation. The frictional pressure drop and liquid pressure drop multiplier values did not seem to be affected too much from more gas injection for constant liquid flow rates until the falling film annular flow transition region. Despite relatively low gas and liquid flow rates, high liquid pressure drop multiplier values were seen for this flow pattern. None of the correlations were able to produce reasonable results against the falling film data. The error was higher especially for low gas flow rates.

5.2 Conclusions of the Heat Transfer Measurement and Analysis

- The heat transfer characteristic of the bubbly flow was similar to the pressure drop characteristic of this flow pattern. In some flow rates, slightly lower heat transfer values were seen in this regime when compared to their single phase liquid heat transfer values. There was not seen any similar findings in the literature that two phase heat transfer could be less than single phase liquid heat transfer for downward vertical flow. It is obvious that more experimental work is needed for different pipe diameters and fluid combinations to verify this phenomenon. For now, at least our pressure drop data supported this heat transfer characteristic by the perspective of Reynolds analogy. Moreover, upward bubbly

flow heat transfer rates were also significantly higher than downward bubbly flow heat transfer rates. This may express buoyancy as an assisting or an opposing force for this regime. As for pressure drop data, the heat transfer rates were predicted reasonably well by most correlations.

- The heat transfer characteristic of slug flow for higher liquid flow rates were quite straight forward. Once again, we observed a highly non linear behavior for low flow rates that the heat transfer rates could be enhanced by reducing liquid or gas flow rates. For these low flow rates, the error with respect to the correlations becomes higher. Overall performances of some correlations for this regime were quite reasonable with the exception of a few points.
- We observed a slight and an almost linear increase in terms of heat transfer by introducing more gas into the system in the froth flow regime. Relatively speaking, it was seen that this regime was not too sensitive to the gas flow unlike the slug flow regime. Consequently, some correlations were quite successful in this regime.
- A monotonic behavior was seen in terms of two phase heat transfer rates in annular flow. Very high amount of gas was needed to increase heat transfer rates in this regime due to the small changes of void fractions. We do not know if there would be further complications related to annular mist transition or very high void fractions due to experimental limitations. Several correlations were able to produce acceptable results for this regime.
- Some unexpected increases and decreases were observed in the two phase heat transfer trend in the falling film flow. So, this regime can be very sensitive to

further liquid or gas injections. One of the reasons could be attributed to the unstable structure of this regime since this regime is under the influence of multiple forces. If we neglect these up and downs in heat transfer rates, an almost horizontal trend can be seen similar to the pressure drop data that one could think that the heat transfer rates were not affected so much by introducing more gas into the system. Another reason of this unexpected behavior of the heat transfer in this regime must be the dry spots problem for some flow rates. If the dry spot problem occurs, the Reynolds analogy will probably fail. This is the only exception for our overall data since all regions showed that downward two phase heat transfer was a very good candidate for Reynolds analogy. Several correlations did well and were able to predict the falling film data reasonably well unlike the pressure drop data.

5.3 Recommendations for Future Experimental Pressure Drop Studies

- As it is seen in the present study, the behavior of two phase flow in vertical orientation is even more complex than horizontal orientation due to the stronger influence of gravity force. Moreover, downward orientation can behave even more nonlinearly due to the direction of flow to which buoyant force acts against. Therefore, pressure drop data should be collected systematically to make a comprehensive analysis. Otherwise, it is very difficult to notice and show the trend of the pressure drop for different regimes since the behavior of the pressure drop can be very sensitive to flow rates in some regions. Although there are some experimental studies for two phase pressure drop in downward orientation in the literature, some data consisted of arbitrary points which do not provide useful

material to present and compare the trend of different regimes. Consequently, the flow rates should be chosen and arranged carefully during the experiment.

- Beside flow rates, the effects of the pipe diameter and working fluid pair are another important issue that must be worked on. Since most correlations generally can produce some reasonable results only for the data of correlation's developer, the choice of the pipe diameter and working fluid pair becomes very important. Since the two phase flow is under the influence of multiple factors, it would be wise to keep some parameters same as other researchers'. For instance, instead of selecting these parameters arbitrarily, one can conduct an experiment by using same pipe size and flow rates that were used in a previous study but for a different working fluid pair. In another word, studies should be related to each other and progress step by step. As we mentioned earlier in the previous chapter, the dimensionless numbers developed for single phase flow analysis were not sufficient to show and explain the behavior of the two phase flow. For example, the effects of velocity, density, diameter, and viscosity on the flow are not exactly clear and grouping these parameters in the form of Reynolds number does not look sufficient. This is the reason why we need to advance step by step and need to see the effects of these parameters separately. By that way, a good mathematical model or correlation can be developed; otherwise, we will continue to work with limited solutions that are developed for specific conditions.
- Lastly, the effect of roughness is another interesting topic that may draw attention for two phase flow. Until now, the influence of the roughness on the two phase flow is not fully understood. Since the shape of velocity profile can be very

different in two phase flow and there are some special flow patterns that manifest themselves as film layers like annular and falling film regimes, the effect of roughness on two phase flow cannot be expected to be same as the one on single phase flow.

5.4 Recommendations for Future Experimental Heat Transfer Studies

- Beside the recommendations made previously for pressure drop, there are several issues that may need to be focused on for future heat transfer studies. The first one may be expressed as the effect of laminar flow. Unlike single phase pressure drop, single phase heat transfer rate is affected from natural convection which causes secondary flow. The effect of secondary flow can be more significant in our case since the gravity force is parallel to the flow direction. For two phase heat transfer, there are some patterns that can be formed only for very low liquid flow rates. If gas flow rates are low too, we do not expect turbulence due to the mixing. Therefore, one may argue the effect of natural convection. Even if natural convection can be negligible, there is a question related to the ratio of two phase heat transfer to superficial single phase heat transfer. Since this ratio concept is used extensively to understand and model two-phase heat transfer, it can be misleading for some flow patterns due to the laminar superficial flow. This is a common problem for two phase heat transfer correlations. Consequently, instead of using turbulent single phase heat transfer correlations to express single phase heat transfer, it could be favorable to measure these laminar single phase heat transfer rates before two phase measurements.

- As it is known, very high heat transfer rates can be observed in annular regime in spite of low liquid flow rates. At the same time, uncertainty is higher for this regime and it is supposed to increase even more by introducing more gas into the system. To deal with this problem, current can be increased. However, due to higher wall temperature, possible local boiling near the pipe wall is an obstacle for researchers. If one would like to conduct experiments and study in detail especially for annular flow regime, fluids that have higher boiling temperature points can be considered to minimize the limitations related to this problem. This will allow obtaining more reliable data while working in extreme regions of annular flow regime.
- Lastly, if it is possible, flow visualization of each run could be very useful for both pressure drop and/or heat transfer in terms of developing a mathematical model.

REFERENCES

Aggour, M.A., (1978), "Hydrodynamics and Heat Transfer in Two-Phase Two-Component Flow", Ph.D. Dissertation, University of Manitoba, Canada.

Beattie, D.R.H., Whalley, P.B., (1982), "A Simple Two-phase frictional Pressure Drop Calculation Method", Int. J. Multiphase Flow, vol. 8, pp. 83–87.

Beggs, D. H., (1972), "An Experimental Study of Two-phase Flow in Inclined Pipes", PhD Dissertation, The University of Tulsa.

Beggs, D. H. and Brill, J. P., (1973), "A Study of Two-phase Flow in Inclined Pipes", Journal of Petroleum Technology, vol. 25, no. 5, pp. 607-617.

Bergelin, O. P., Kegel, P. K., Carpenter, F. G. and Gazley, C., (1949), "Co-Current Gas-Liquid Flow, Flow in Vertical Tubes", ASME Heat Transfer and Fluid Mechanics Institute,Berkeley, California, pp.19-28, June.

Bhagwat, S., (2011), "Study of Flow Patterns and Void Fraction in Vertical Downward Two-phase Flow", Master Thesis, Oklahoma State University, Stillwater.

Chilton T.H. and Colburn A.P., (1934),. "Mass Transfer (Absorption) Coefficients Prediction from Data on Heat Transfer and Fluid Friction", Industrial and Engineering Chemistry, vol. 26, pp. 1183-1187.

Chisholm, D. (1967), "A Theoretical Basis for The Lockhart-martinelli Correlation for Two-phase Flow", International Journal of Heat and Mass Transfer, vol. 10, no. 12, pp.1767-1778.

Churchill, S.W., (1977), "Friction-factor Eqution Spans All Fluid-flow Regimes", Chemical Engineering, vol. 84, no. 24, pp. 91-92.

Chu, Y.C. and Jones, B.G., (1980), "Convective Heat Transfer Coefficient Studies in Upward and Downward Vertical Two-Phase Non-Boiling Flows", AIChE. 7: pp. 79-90.

Cicchitti, A., Lombardi, C., Silvestri, M., Soldaini, G. and Zavattarelli, R., (1960), "Two-phase Cooling Experiments: Pressure drop, Heat transfer and Burnout Measurements", Energia Nucleare, vol. 7, no. 6, pp. 407-425.

Colebrook, C.F. (1939)., "Turbulent Flow in Pipes, with Particular Reference to the Transition Region Between Smooth and Rough Pipe Laws", Proc. Institution of Civil Engineers, vol. 12, pp. 393-422.

Cook, W. L., (2008), "An Experimental Apparatus for Measurement of Pressure Drop, Void Fraction, and Non-boiling Two-phase Heat transfer and Flow Visualization in Pipes for All Inclinations", Master Thesis, Oklahoma State University, Stillwater.

Dittus, F. W. and Boelter, L. M. K., (1930), "Heat Transfer Inautomobile Radiators of The Tubular Type", University of California Publications in Engineering, vol. 2, pp. 443-461.

Drucker, M.I., Dhir, V.K., and Duffey, R.B., (1984), "Two Phase Heat Transfer for Flow in Tubes and Over Rod Bundles with Blockages", Trans. of ASME, J. of Heat Transfer, vol. 106, pp. 856-864.

Dorresteijn, W.R., (1970), "Experimental Study of Heat Transfer in Upward and Downward Two Phase Flow of Air and Oil through 700 m Tubes", Proccedings of the 4th International Heat Transfer Conference.

Dukler, A. E., Wicks, M. and Cleveland, R. G. (1964), "Frictional Pressure Drop in Two-phase Flow: Part A and B", AIChE Journal, vol. 10, no. 1, pp.38-51.

Ghajar, A. J. and Kim, J., (2006) “Calculation of Local Inside-Wall Convective Heat Transfer Parameters from Measurements of the Local Outside-Wall Temperatures along an Electrically Heated Circular Tube”, Heat Transfer Calculations, edited by Myer Kutz, McGraw-Hill, New York, NY, pp. 23.3-23.27,

Ghajar, A. J. and Tam, L. M., (1994), "Heat Transfer Measurements and Correlations in the Transition Region for a Circular Tube with Three Different Inlet Configurations", Experimental Thermal and Fluid Science, vol. 8, no. 1, pp. 79-90.

Ghajar, A. J. and Zurigat, Y. H., (1991), "Microcomputer-Assisted Heat Transfer Measurements/Analysis in a Circular Tube", International Journal of Applied Engineering Education, vol. 7, no. 2, pp. 125-134.

Gnielinski, V., (1976), "New Equations for Heat and Mass Transfer in Turbulent Pipe and Channel Flow", International Chemical Engineering, vol. 16, pp. 359-368.

Hajiloo, M., Chang, B.H., and Mills, A.F., (2001), "Interfacial Shear in Downward Two-phase Annular Co-current Flow", International Journal of Multiphase Flow. Vol. 27: pp. 1095-1108.

Katasuhara, T. and Kazama, T., (1958), "Heat Transfer in Two Phase Flow of Mixtures of Air-water", Trans. of JSME, 2nd Report, Vertical Channel, vol. 24: pp. 552-558.

Khoze, A.N., Dunayev, S.V., and Sparin, V.A., (1976), "Heat and Mass Transfer in Rising Two-Phase Flows in Rectangular Channels", Heat Transfer - Soviet Research, vol. 8, no. 3, pp. 87-90.

Kim, D., Ghajar, A.J., and Dougherty, R.L., (2000), "Robust Heat Transfer Correlation for Turbulent Gas-Liquid Flow in Vertical Pipes", Journal of Thermophysics and Heat Transfer, vol. 14, no. 4, pp. 574-578.

Kline, S. J. and F. A. McClintock., (1953), "Describing Uncertainties in Single-Sample Experiments", Mechanical Engineering, vol. 75, pp. 3-8.

Knott, R.F., Anderson, R.N., Acrivos, A., and Petersen, E.E.,(1959), "An Experimental Study of Heat Transfer to Nitrogen-Oil Mixtures", Industrial and Engineering Chemistry, Process Design and Development, vol. 51, no. 11, pp.1369-1372.

Kudirka, A.A., Grosh, R.J., and McFadden, P.W., (1965), "Heat Transfer in Two Phase Flow of Gas-Liquid Mixtures", I&EC Fndamentals, vol. 4, no. 3, pp. 329-334.

Linstrom, P. J., and Mallard, W. G., (eds.) (2003), NIST ChemistryWebBook, NIST Standard Reference Database No. 69, National Institute of Standards and Technology, http://webbook.nist.gov .

Lockhart, R. W. and Martinelli, R. C. (1949), "Proposed Correlation of Data for Isothermal Two-phase, Two component Flow in Pipes", Chemical Engineering Progress, vol. 45, no. 1, pp.39-48.

Martinelli, R.C., Boelter, L.M.K., Taylor, T.H.M., Thomsen, E.G. and Morrin, E.H., (1944), “Isothermal Pressure Drop for Two-phase, Two-component Flow in a Horizontal pipe”, Trans. ASME, vol. 66, pp. 139-151.

McAdams, W. H., Woods, W. K. and Heroman, L. C. (1942), "Vaporization Inside Horizontal Tubes – II - Benzene-oil Mixtures", Trans. ASME, vol. 64, no. 3, pp.193-200.

Mukherjee, H. (1979), "An Experimental Study of Inclined Two-phase Flow", PhD Dissertation, The University of Tulsa.

Ravipudi, S.R. and Godbold, T.M., (1978), "The Effect of Mass Transfer on Heat Transfer Rates for Two-Phase Flow in Vertical Pipe", Proc. of the 6th International Heat Transfer Conference, Toronto, Canada, vol.1, pp. 505-510.

Rezkallah, K.S. and Sims, G.E., (1987), "An Examination of Correlations of Mean Heat Transfer Coefficients in TwoPhase and two-Component Flow in Vertical Tubes", AIChE Symp. Series 83, pp. 109-114.

Oshinowo, O., (1971), "Two Phase Flow in a Vertical Tube Coil". Ph.D. Dissertation, University of Toronto, Toronto.

Oshinowo, O., Betts, R.C., and Charles, M.E., (1984), "Heat Transfer in Co-current Vertical Two Phase Flow", Canadian Journal of Chemical Engineering, vol. 62, pp. 194-199.

Shah, M.M., (1981), "Generalized Prediciton of Heat Transfer during Two-Component Gas-Liquid Flow in Tubes and Other Channels", AIChE Symp. Series. **77**, pp. 140-151.

Shannak, B. A. (2008), "Frictional Pressure Drop of Gas Liquid Two-phase Flow in Pipes", Nuclear Engineering and Design, vol. 238, no. 12, pp. 3277-3284.

Sieder, E.N. and G.E. Tate (1936), “Heat Transfer and Pressure Drop of Liquids in Tubes”, Industrial and Engineering Chemistry, vol. 28, pp. 1429-1435.

Sun, L. and Mishima, K. (2009), "Evaluation Analysis of Prediction Methods for Two-phase Flow Pressure Drop in Mini-channels", International Journal of Multiphase Flow, vol. 35, no. 1, pp.47-54.

Tang, C.C. and Ghajar, A.J., (2007), "Validation of a General Heat Transfer Correlation for Non-Boiling Two-Phase Flow with Different Flow Patterns and Pipe Inclination Angles", Proceedings of the 2005 ASME-JSME Thermal Engineering Heat Transfer Connference. Vancouver, Canada: July 8-12.

Tang, C.C. and Ghajar, A.J., (2011), "A Mechanistic Heat Transfer Correlation for Non-Boiling Two-Phase Flow in Horizontal, Inclined and Vertical Pipes", Proceedings of AJTEC 2011 ASME/JSME 8th Thermal Engineering Joint Conference, Hawaii, USA: Paper No. AJTEC2011-44114.

Ueda, T. and Kanaoka, M., (1967), "On Upward Flow of Gas Liquid Mixtures in Vertical Tubes", Heat Transfer Results and Analysis, Bulletin JSME, vol. 10, pp. 1008-1015.

Vijay, M.M., Aggour, M.A., and Sims, G.E., (1982), "A Correlation of Mean Heat Transfer Coefficients for Two-Phase Two-Component Flow in a Vertical Tube", Proceedings of the 7th International Heat Transfer Conference, Munich, Germany.

Yamazaki, Y. and Yamaguchi, K., (1979), "Characteristics of Co-current Two-phase Downflow in Tubes- Flow pattern, Void fraction and Pressure Drop", Journal of Nuclear Science and Technology, vol. 16, pp. 245-255.

Webb, D.R., and Hewitt, G.F., (1975), "Downward Co-current Annular Flow", Int. J. Multiphase Flow, vol. 2, no. 1, pp. 35-49.

APPENDIX A

UNCERTAINTY ANALYSIS

A.1 Pressure Drop

A.1.1 Single Phase Flow

It is better to calculate uncertainty in terms of friction factor due to its widely acceptance in engineering community. The Darcy friction factor is defined as follows:

$$f = \frac{2D\Delta P}{\rho L U^2} = \frac{\Delta P D^5 \pi^2 \rho}{8L^2} \tag{A.1}$$

It can be easily seen that the friction factor is a function of five parameters. Kline&McClintock (1953) method can be used for the analysis.

$$w_R = [\left(\frac{\partial R}{\partial x_1} w_1\right)^2 + \left(\frac{\partial R}{\partial x_2} w_2\right)^2 + \cdots + \left(\frac{\partial R}{\partial x_n} w_n\right)^2]^{1/2} \tag{A.2}$$

Then, the uncertainty of single phase friction factor becomes:

$$w_f = [\left(\frac{\partial f}{\partial \Delta P} w_{\Delta P}\right)^2 + \left(\frac{\partial f}{\partial \rho} w_\rho\right)^2 + \left(\frac{\partial f}{\partial L} w_L\right)^2 + \left(\frac{\partial f}{\partial} w\right)^2 + \left(\frac{\partial f}{\partial D} w_D\right)^2]^{1/2} \tag{A.3}$$

If we divide both sides by friction factor, we will get percentage uncertainty:

$$\frac{w_f}{f} = [\left(\frac{1}{\Delta P} w_{\Delta P}\right)^2 + \left(\frac{1}{\rho} w_\rho\right)^2 + \left(\frac{1}{L} w_L\right)^2 + \left(\frac{2}{} w\right)^2 + \left(\frac{5}{D} w_D\right)^2]^{1/2} \tag{A.4}$$

The uncertainty values related to the parameters in the above equation and a sample calculation for single phase pressure drop are given in the Tables A.1 and A.2, respectively:

Table A.1 Uncertainty Values Related to the Parameters

Instrument/Method	Parameter	Uncertainty
Validyne Pressure Transducer	Pressure Drop(ΔP)	±0.25%
Fitted Equation (Linstrom&Mallard (2003))	Density(ρ)	±0.06%
Dial Calipers	Length(L)	±1.27E-05 m
MicroMotion Coriolis Flow Meter	Mass Flow Rate( )	±1.8%
Dial Calipers	Diameter(D)	±1.27E-05 m

Table A.2 Single Phase Pressure Drop Sample Calculation (Run 0001, Re_{SL} = 34238)

Variable	Value	Uncertainty	Uncertainty%
Length(L)	0.889 m	±1.27E-05 m	±0.001%
Diameter(D)	0.01252 m	±1.27E-05 m	±0.10%
Density(ρ)	997.24 kg/m^3	±0.6 kg/m^3	±0.06%
Mass Flow Rate( )	0.307 kg/s	±0.0055 kg/s	±1.8%
Pressure Drop(ΔP)	5591 Pa	±13.98 Pa	±0.25%
Friction Factor(f)	0.0253	±0.00092	±3.6%

A.1.2 Two Phase Flow

There is not a common two phase friction factor description. Different definitions of friction factor lead to different uncertainties. Before going for a two phase friction factor uncertainty, we introduce an uncertainty analysis for frictional pressure.

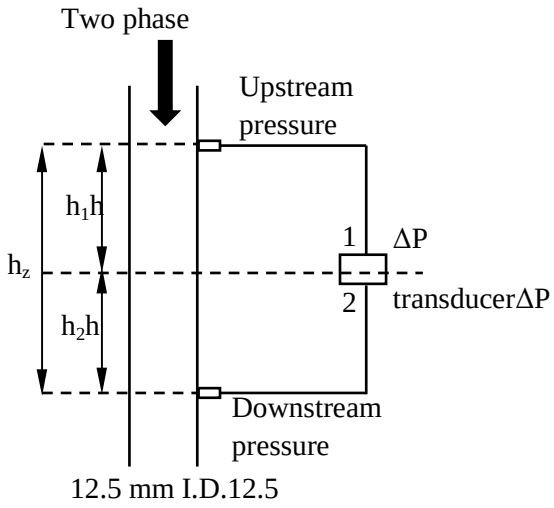

Figure A.1 Schematic of Differential Pressure Transducer System

The pressure drop due to acceleration can be negligible for short pipes. Thus, an equation can be written with reference to the figure as follows (Figure A.1):

$$P_2 = P_1 - \rho_L h_1 g + \rho_M h_1 g + \rho_M h_2 g - \rho_L h_2 g - \Delta P_{Frictional} \quad \text{(A.5)}$$

where the mixture density is calculated from:

$$\rho_M = \alpha \rho_G + (1 - \alpha)\rho_L \quad \text{(A.6)}$$

If we simplify and rearrange, we get:

$$\Delta P_{Frictional} = P_1 - P_2 - (\rho_L - \rho_G)(h_1 + h_2)\alpha g$$

$$= \Delta P_{Measured} - (\rho_L - \rho_G)(h_1 + h_2)\alpha g \quad \text{(A.7)}$$

Please notice that $\Delta P_{Measured}$ is not the total pressure drop but the pressure difference between the pressure transducer's tips. The total pressure drop can also be calculated if it is needed.

$$\Delta P_{Total} = \Delta P_{Measured} - \rho_L(h_1 + h_2)g \quad \text{(A.8)}$$

Moreover, as it can be seen, there is no need to calculate hydrostatic pressure drop for single phase since $\alpha = 0$.

The problem related to calculation of frictional two phase pressure drop in vertical flows is the accuracy of void fraction. Since the equation is very sensitive to void fraction, it is better to measure pressure drop and void fraction simultaneously. Another way is using accurate void fraction correlations. In this work, void fraction is calculated from suitable void fraction correlations. Bhagwat (2011) provided a criteria for selection of the void fraction correlations since both Bhagwat (2011) and the present study was conducted on the same experimental setup and same mass flow rates range was analyzed. This ensured which correlation was suitable for different flow patterns and void fraction ranges for the present work. Thus, the uncertainty related to void fraction is directly linked to the performance of the void fraction correlations for the present study.

Now, if we return to the equation and use Kline&McCLintock (1953) method for frictional pressure drop,

$$w_{\Delta P_{Frictional}} =$$

$$\left[\left(\frac{\partial \Delta P_{Frictional}}{\partial \Delta P_{Measured}} w_{\Delta P_{Measured}}\right)^2 + \left(\frac{\partial \Delta P_{Frictional}}{\partial \rho_L} w_{\rho_L}\right)^2 + \left(\frac{\partial \Delta P_{Frictional}}{\partial \rho_G} w_{\rho_G}\right)^2 + \left(\frac{\partial \Delta P_{Frictional}}{\partial h_z} w_{h_z}\right)^2 + \left(\frac{\partial \Delta P_{Frictional}}{\partial \alpha} w_{\alpha}\right)^2\right]^{1/2} \quad \text{(A.9)}$$

Then, the percentage uncertainty becomes:

$$\frac{w_{\Delta P_{Frictional}}}{\Delta P_{Frictional}} =$$

$$\left[\left(\frac{1}{\Delta P_{Measured} - (\rho_L - \rho_G) h_z \alpha g} w_{\Delta P_{Measured}}\right)^2 + \left(\frac{-h_z \alpha g}{\Delta P_{Measured} - (\rho_L - \rho_G) h_z \alpha g} w_{\rho_L}\right)^2 + \left(\frac{h_z \alpha g}{\Delta P_{Measured} - (\rho_L - \rho_G) h_z \alpha g} w_{\rho_G}\right)^2 + \left(\frac{-g\alpha(\rho_L - \rho_G)}{\Delta P_{Measured} - (\rho_L - \rho_G) h_z \alpha g} w_{h_z}\right)^2 + \left(\frac{-g h_z (\rho_L - \rho_G)}{\Delta P_{Measured} - (\rho_L - \rho_G) h_z \alpha g} w_{\alpha}\right)^2\right]^{1/2} \quad \text{(A.10)}$$

The uncertainties related to frictional pressure drop based on different flow patterns and sample calculation for the bubbly flow are given in the Tables A.3 and A.4, respectively. All points in each flow pattern except few points were within the given uncertainty range.

Table A.3 Frictional Pressure Drop Uncertainties Based on Different Flow Patterns

Flow Pattern	**Min. Uncertainty %**	**Max. Uncertainty %**
Bubbly	1.95	9.4
Slug	2.57	10.47
Froth	2.63	1.26
Falling Film	2.84	5.57
Annular	1.02	3.78

Table A.4 Two Phase Pressure Drop Sample Calculations (Run 0004, Bubbly Flow)

Variable	Value	Uncertainty	Uncertainty%
h_z	0.889 m	±1.27E-05 m	±0.001%
ρ_L	996.83 kg/m^3	±0.598 kg/m^3	±0.06%
ρ_G	1.48 kg/m^3	±0.0009 kg/m^3	±0.06%
α	0.091	±0.009	±10%
$\Delta P_{Measured}$	1937.08 Pa	4.84 Pa	±0.25%
$\Delta P_{Frictional}$	1149.15 Pa	79	±6.9%

It is also possible to make an uncertainty analysis based on two phase friction factor.

$$f_{TP} = \frac{\Delta P_{Frictional} D^5 \pi^2 \rho_{TP}}{8L(_L+_G)^2} = \frac{(\Delta P_{Measured} - (\rho_L - \rho_G)\alpha h_z g) D^5 \pi^2 \rho_{TP}}{8L(_L+_G)^2} \quad \text{(A.11)}$$

Now, ρ_{TP} should be defined. A suitable way is to use quality dependent definition since most correlations are based on this definition.

$$\rho_{TP} = \frac{1}{\frac{x}{\rho_G} + \frac{1-x}{\rho_L}} = \frac{1}{\frac{G/_{Total}}{\rho_G} + \frac{1-G/_{Total}}{\rho_L}} \quad \text{(A.12)}$$

If we introduce ρ_{TP} into the equation and simplify, we get:

$$f_{TP} = \frac{(\Delta P_{Measured} - (\rho_L - \rho_G)\alpha h_z g) D^5 \pi^2}{8L[\frac{G(G+L)}{\rho_G} - \frac{G(G+L)}{\rho_L} + \frac{(G+L)^2}{\rho_L}]} \quad \text{(A.13)}$$

Consequently, an uncertainty for f_{TP} can be found similar to single phase friction factor.

$$w_{f_{TP}} = [\left(\frac{\partial f_{TP}}{\partial \Delta P_{Measured}} w_{\Delta P_{Measured}}\right)^2 + \left(\frac{\partial f_{TP}}{\partial \rho_L} w_{\rho_L}\right)^2 + \left(\frac{\partial f_{TP}}{\partial \rho_G} w_{\rho_G}\right)^2 +$$

$$\partial f TP \partial hz whz2 + \partial f TP \partial \square Lw \square L2 + \partial f TP \partial \square Gw \square G2 + \partial f TP \partial Dw D2 + \partial f TP \partial \alpha w \alpha 2]1/2$$

(A.14)

A.2 Heat Transfer

The heat transfer coefficient is defined as follows:

$$h = \frac{\dot{q}''}{\bar{T}_{wi} - \bar{T}_b} \tag{A.15}$$

Then, the uncertainty becomes:

$$w_h = [\left(\frac{\partial h}{\partial \dot{q}''} w_{\dot{q}''}\right)^2 + \left(\frac{\partial h}{\partial \Delta T} w_{\Delta T}\right)^2]^{\frac{1}{2}} = [\left(\frac{1}{\Delta T} w_{\dot{q}''}\right)^2 + \left(\frac{-\dot{q}''}{\Delta T^2} w_{\Delta T}\right)^2]^{1/2} \tag{A.16}$$

The uncertainty for ΔT can be assumed to be the sum of the uncertainties of inner average wall temperature and the average bulk temperature. The average inner wall temperature is defined as follows:

$$\bar{T}_{wi} = \dot{q} R_t + \bar{T}_{wo} \tag{A.17}$$

Then, the uncertainty associated with the average inner wall temperature becomes:

$$w_{\bar{T}_{wi}} = [(R_t w_{\dot{q}})^2 + (\dot{q} w_{R_t})^2 + (w_{\bar{T}_{wo}})^2]^{1/2} \quad \text{(A.18)}$$

Please also notice that the uncertainty of the average outer wall temperature can be assumed as 0.5℃ since it is the average of 28 thermocouples.

The thermal resistance is given as:

$$R_t = \frac{\ln(\frac{D_o}{D_i})}{2\pi k L} \quad \text{(A.19)}$$

And the uncertainty related to the thermal conduction becomes:

$$w_{R_t} = [(\frac{1}{2\pi D_o k L} w_{D_o})^2 + (\frac{-1}{2\pi D_i k L} w_{D_i})^2 + (\frac{-\ln(\frac{D_o}{D_i})}{2\pi k^2 L} w_k)^2 + (\frac{-\ln(\frac{D_o}{D_i})}{2\pi L^2 k} w_L)^2]^{1/2} \quad \text{(A.20)}$$

The uncertainties of the heat transfer rate and the heat flux can be obtained by a similar approach.

$$\dot{q} = VI \quad \text{(A.21)}$$

$$w_{\dot{q}} = [(I w_V)^2 + (V w_I)^2]^{1/2} \quad \text{(A.22)}$$

$$\dot{q}'' = \frac{VI}{\pi D_i L} \quad \text{(A.23)}$$

$$w_{\dot{q}''} = [(\frac{I}{\pi D_i L} w_V)^2 + (\frac{V}{\pi D_i L} w_I)^2 + (\frac{-VI}{\pi {D_i}^2 L} w_{D_i})^2 + (\frac{-VI}{\pi D_i L^2} w_L)^2]^{1/2} \quad \text{(A.24)}$$

The heat balance error associated with the run should also be added to the heat transfer rate error. Finally Tables A.5, A.6 and A.7 show uncertainty sample heat transfer

calculations for single phase, two-phase slug flow and two-phase uncertainties based on flow patterns, respectively.

Table A.5 Single Phase Heat Transfer Sample Calculations (Run=0001)

Variable	Value	Uncertainty	Uncertainty%
Inner Diameter(D_i)	0.0125 m	±1.27E-05 m	±0.10%
Outer Diameter(D_o)	0.0171 m	±1.27E-05 m	±0.07%
Length (L)	1.016 m	±3.175E-03 m	±0.31%
Thermal Conductivity(k)	13.438W/mK	-	-
Ampere(I)	506 A	±5.06 A	±1.00%
Voltage(V)	3.5 V	±0.35 V	±1.00%
Thermal Resistance(R_t)	0.0036 K/W	±2.177E-05 m	±0.6%
Average Inner Wall Temp. ($\bar{T}_{wi}$)	39.05℃	0.59℃	±1.52%
$\bar{T}_{wi}$ -$\bar{T}_b$ (ΔT)	17.77℃	1.09℃	±6.14%
Heat Balance Error	-	-61.75 W	-3.48%
Heat Transfer Rate($\dot{q}$)	1772.15 W	±25.07 W	±1.41%
Heat Flux($\dot{q}''$)	44337.9 W/m^2	±644.08	±1.45%
Heat Transfer Coefficient(h)	2587.9 W/m^{2}K	±157.5	±6.1%

Table A.6 Two Phase Heat Transfer Sample Calculations (Run=0048, Slug Flow)

Variable	Value	Uncertainty	Uncertainty%
Inner Diameter(D_i)	0.0125 m	±1.27E-05 m	±0.10%
Outer Diameter(D_o)	0.0171 m	±1.27E-05 m	±0.07%
Length (L)	1.016 m	±3.175E-03	±0.31%
Thermal Conductivity(k)	13.438W/mK	-	-
Ampere(I)	575.08 A	±5.75 A	±1.00%
Voltage(V)	3.96 V	±0.396 V	±1.00%
Thermal Resistance(R_t)	0.0036 K/W	±2.177E-05	±0.6%
Average Inner Wall Temp. ($\bar{T}_{wi}$)	38.34℃	0.94℃	±2.46%
$\bar{T}_{wi}$ -$\bar{T}_b$ (ΔT)	16.48℃	1.44℃	±8.75%
Heat Balance Error	-	-186.9 W	-8.22%
Heat Transfer Rate($\dot{q}$)	2274.76 W	±32.2 W	±1.42%
Heat Flux($\dot{q}''$)	569129.9 W/m^2	±827.38	±1.45%
Heat Transfer Coefficient(h)	3599.64 W/m^{2}K	±306.3	±8.51%

Table A.7 Two Phase Heat Transfer Uncertainties Based on Flow Pattern

Flow Pattern	**Min. Uncertainty %**	**Max. Uncertainty %**	**Avg. Uncertainty %**
Bubbly	3.04	7.76	6.28
Slug	3.73	6.55	4.8
Froth	6.1	8.4	7.4
Falling Film	7.4	12.7	10.0
Annular	10.3	13.3	12.2

VITA

Mehmet Mollamahmutoglu

Candidate for the Degree of

Master of Science in Mechanical Engineering

Thesis: STUDY OF ISOTHERMAL PRESSURE DROP AND NON-BOILING HEAT TRANSFER IN VERTICAL DOWNWARD TWO PHASE FLOW

Major Field: Mechanical Engineering

Biographical:

Education:

Completed the requirements for the Master of Science in Mechanical Engineering at Oklahoma State University, Stillwater, Oklahoma in December, 2012.

Completed the requirements for the Bachelor of Science in Mechanical Engineering at Gazi University, Ankara, Turkey in 2009.